ÇUKUROVA UNIVERSITY
INSTITUTE OF NATURAL AND APPLIED SCIENCES

MSc THESIS

Ebru ŞENYİĞİT SİNEKLİ

DYNAMIC INTEGRAL SLIDING MODE CONTROL OF AN ELECTROMECHANICAL SYSTEM

DEPARTMENT OF COMPUTER ENGINEERING

ADANA-2018

ÇUKUROVA UNIVERSITY
INSTITUTE OF NATURAL AND APPLIED SCIENCES

DYNAMIC INTEGRAL SLIDING MODE CONTROL OF AN ELECTROMECHANICAL SYSTEM

Ebru ŞENYİĞİT SİNEKLİ

MSc THESIS

DEPARTMENT OF COMPUTER ENGINEERING

We certify that the thesis titled above was reviewed and approved for the award of degree of the Master of Science by the board of jury on 29/05/2018

…………………………………….	……………………………………….	………………………………………………..
Assoc. Prof. Dr. Ramazan ÇOBAN	Asst. Prof. Dr. B.Melis ÖZYILDIRIM	Asst. Prof. Dr. İpek ABASIKELEŞ TURGUT
SUPERVISOR	MEMBER	MEMBER

This MSc Thesis is written at the Department of Institute of Natural And Applied Sciences of Çukurova University.
Registration Number:

Prof. Dr. Mustafa GÖK
Director
Institute of Natural and Applied Sciences

This study was supported by Research Projects Unit Ç.Ü. Project Number: FYL-2016-6612

DEDICATION

… to my unborn son Deniz Ayaz, my mom and my husband

ABSTRACT

MSc THESIS

DYNAMIC INTEGRAL SLIDING MODE CONTROL OF AN ELECTROMECHANICAL SYSTEM

Ebru ŞENYİĞİT SİNEKLİ

ÇUKUROVA UNIVERSITY
INSTITUTE OF NATURAL AND APPLIED SCIENCES
DEPARMENT OF COMPUTER ENGINEERING

Supervisor : Assoc. Prof. Dr. Ramazan ÇOBAN
Year : 2018, Pages: 61
Jury : Assoc. Prof. Dr. Ramazan ÇOBAN
: Asst. Prof. Dr. Buse Melis ÖZYILDIRIM
: Asst. Prof. Dr. İpek ABASIKELEŞ TURGUT

In this study, a new dynamic integral sliding mode control is put forward to control the speed of an electromechanical system. The dynamic integral sliding mode control is proposed to make sliding mode control aspects better and remove undesirable chattering effects. Lyapunov stability theorem is applied to guarantee the system's stability. The output speed, the sliding surface, and the control input of the electromechanical system for the controllers are examined. The simulation and experimental results obtained from the conventional sliding mode control are compared with the simulation and experimental results of the proposed dynamic integral sliding mode control under none, 20% and 80% of parameter uncertainty. The dynamic integral sliding mode control is much more robust than the conventional sliding mode control with respect to parameter variations.

Key Words: Sliding Mode Control; Dynamic Integral Sliding Mode Control; DC Servo Motor; Chattering; Parameter Uncertainty.

ÖZ

YÜKSEK LİSANS TEZİ

DYNAMIC INTEGRAL SLIDING MODE CONTROL FOR AN ELECTROMECHANICAL SYSTEMS

Ebru ŞENYİĞİT SİNEKLİ

ÇUKUROVA ÜNİVERSİTESİ
FEN BİLİMLERİ ENSTİTÜSÜ
BİLGİSAYAR MÜHENDİSLİĞİ ANABİLİM DALI

Danışman : Doç. Dr. Ramazan ÇOBAN
Yıl: 2018, Sayfa: 61
Jüri : Doç. Dr. Ramazan ÇOBAN
: Dr. Öğr. Üyesi Buse Melis ÖZYILDIRIM
: Dr. Öğr. Üyesi İpek ABASIKELEŞ TURGUT

Bu çalışmada bir elektromekanik sistemin hızını kontrol edebilmek için yeni bir kontrol metodu olan dinamik integral kayan kipli kontrol metodu geliştirildi. Dinamik integral kayan kipli kontrol yöntemi, geleneksel kayan kipli kontrol yönteminin özelliklerini iyileştirmek ve geleneksel kayan kipli kontrolün en büyük sıkıntılarından biri olan çatırdama problemini ortadan kaldırmak için önerildi. Sistemin kararlılığı Lyapunov kararlılık teoremi ile sağlandı. Dinamik kayan kipli kontrol ve geleneksel kayan kipli kontrol gerçek zamanlı sistem üzerine uygulanmış, %20 ve %80 parametre belirsizlikleri altında sistemin başarısı kıyaslanmıştır. Dinamik kayan kipli kontrol parametre değişimlerine karşı geleneksel kayan kipli kontrolden çok daha fazla gürbüzdür.

Anahtar Kelimeler : Kayan Kipli Kontrol, Dinamik Kayan Kipli Kontrol, DC Servo Motor, Çatırdama, Parametre Belirsizliği.

EXPANDED SUMMARY

In this study, a new dynamic integral sliding mode control is put forward to control the speed of an electromechanical system. Chattering phenomenon is the main problem while implementing the conventional SMC to the electromechanical system. In this thesis, the new dynamic integral switching function is proposed to remove the chattering effects with good robustness. The integral property is added to the switching function to build more durable system to parameter variations. The dynamic integral sliding mode control is proposed to make sliding mode control aspects better and remove undesirable chattering effects.

Lyapunov theorem is applied to guarantee the system's stability. The system under various parameter uncertainty is considered closer to the real world industrial systems.

The conventional sliding mode control (SMC) is suitable for uncertain nonlinear systems and the popularly used control method which provides high accuracy, robustness, fast response, good transient performance, order reduction and insensitivity to parameter variations against various internal and external perturbations. However, it has undesirable chattering effect on the sliding surface while implementing the conventional SMC for some real world applications. The conventional SMC has been widely expanded to integrate new methods in order to overcome the chattering.

The Dynamic Integral Sliding Mode Control (DISMC) keeps the advantages of the integral sliding mode control and dynamic sliding mode control. The sliding mode is constructed without reaching phase for the integral sliding mode control. Unfortunately, there is a frequently encountered problem which is called chattering in the implementation of the conventional SMC. The dynamic integral sliding mode control overcomes the chattering sufficiently, eliminates the reaching phase and inherits all advantages of the conventional SMC. The DISMC is designed by adding integral property to sliding surface and yielding chatter free

control with the desired performance. It is robust control method with respect to parameter variations and imprecisions

The simulation and experimental results obtained from the conventional sliding mode control are compared with the simulation and experimental results of the proposed dynamic integral sliding mode control under none, 20% and 80% of parameter uncertainty. Experimental results verify that dynamic integral sliding mode control method provides preferable tracking performance, overcomes chattering, and has better raising time, smaller settling time, and no overshoot. It is robust with respect to parameter variations compared to sliding mode control.

Some experimental applications of the conventional SMC and the DISMC are implemented to the real electromechanical system to show their effectiveness. The rotor speeds, the system sliding surfaces and the control signals for the conventional SMC and the proposed DISMC are investigated. Different uncertainty parameter values are applied to the system to test the robustness of the system.

The DISMC is more efficient control method compared with the conventional SMC based on both a simulation program environment and the experimental results. Hence, the DISMC should be used in industrial systems alternatively because usage of it is simple, easy to implement, its robustness and performance are more effective than the conventional SMC. According to both the experimental results and a simulation program results, the robustness and the control performance of the system with the DISMC have been significantly increased.

The DISMC is more efficient, robust against the parameter variations and smooth in the presence of the parameter uncertainty. The DISMC also overcomes the chattering phenomena. The tracking error for the DISMC converges to zero under the parameter uncertainties.

ACKNOWLEDGMENTS

Foremost, I would like to express my sincere gratitude to my advisor Assoc. Prof. Dr. Ramazan ÇOBAN, for his supervision guidance, encouragements, patience, motivation, useful suggestions and his valuable time for this work.

I would like to thank members of the MSc thesis jury, Asst. Prof. Dr. and Asst. Prof. Dr. , for their suggestions and corrections.

I would also like to thank Çukurova University Scientific Research Projects Center for supporting this work (Project no: FYL-2016-6612)**.**

Last but not the least; I would like to thank my family for their endless support and encouragements for my life and my career.

CONTENTS **PAGE**

LIST OF TABLES **PAGE**

LIST OF FIGURES **PAGE**

LIST OF SYMBOLS

t	:	Torque
K_t	:	Torque constant
v_{emf}	:	Induced electromotive force
q&	:	Angular shaft velocity
K_b	:	Motor property dependent constant related to physical properties of the motor
d	:	Viscous friction
$u(t)$	:	Control signal
R	:	Resistance
L	:	Inductance
J	:	Moment of inertia
a,b,c	:	System Parameters
$e(t)$	:	Tracking error
s(t)	:	Sliding Surface
$u_1(t)$	:	Switching Control
$u_0(t)$	:	Equivalent Control
s (t)	:	Dynamic Sliding Surface
$V(t)$	:	Lyapunov Stability Function

LIST OF ABBREVIATIONS

SMC	:	Sliding Mode Control
DSMC	:	Dynamic Sliding Mode Control
DISMC	:	Dynamic Integral Sliding Mode Control
sgn	:	Signum Function
sat	:	Saturation Function

1. INTRODUCTION

From 1978 to present, thousands of studies are published about sliding mode control and its variations. The main concepts, mathematics and design aspects of the conventional sliding mode control (SMC) are first proposed by Utkin (V. I. Utkin 1978). It has shown that SMC can be used for different types of electric motors. SMC is operated to high dimensional nonlinear systems under parametric uncertainty (V. I. Utkin 1978).

Dynamic sliding mode control (DSMC) and high order sliding mode control are compared by Koshkouei et al (Koshkouei, Burnham, and Zinober 2005). Some conditions for reaching trajectories to suitable sliding surface are proposed. Dynamic sliding mode control differentiator is studied. The DSMC has performed much better than the high order sliding mode control (Koshkouei, Burnham, and Zinober 2005).

The chattering problem is explained by Utkin and Lee (V. Utkin and Lee 2006). Two main reasons of chattering which are the unmodeled dynamics and using digital controllers with limited sampling rate are defined. Using asymptotic observer is the most efficient way to remove chattering (V. Utkin and Lee 2006).

The conventional Sliding Mode Control and Dynamic Sliding Mode Control (DSMC) for MIMO three tank system is studied by Iqbal et al (Iqbal, Bhatti, and Khan 2009). The tracking performance of LMI based H_∞ controller is used. Simulation results are given to show effectiveness of the DSMC against the parameter uncertainties and noises (Iqbal, Bhatti, and Khan 2009).

The conventional Sliding Mode Control (SMC) and PID tuning technique with low pass filter are explained to control the DC servo motor motion by Chamsai et al (Chamsai, Jirawattana, and Radpukdee 2010). The chattering is removed by using the boundary layer technique. The SMC gives better performance than PID (Chamsai, Jirawattana, and Radpukdee 2010).

The dynamic sliding mode control for the electro-hydraulic position (EHPS) servo system is proposed by Tang and Zhang (Tang and Zhang 2011). The EHPS system description is explained. The simulation and experimental results are given (Tang and Zhang 2011).

The Dynamic Integral Sliding Mode Control (DISMC) is presented for the flutter suppression of an aeroelastic system with softening spring stiffness by Xue and Li (Xue and Li 2016). The simulation results have shown that the closed loop system using the DISMC has better performance than the backstepping second-order sliding mode control (BSOSMC) (Xue and Li 2016).

The adaptive sliding mode control for nonlinear Markovian jump systems (MJSs) with partly unknown transition probabilities is studied by Li et al (Li et al. 2016). Observer-based adaptive sliding mode controller and an integral sliding mode surface is designed to demonstrate the effectiveness of the MJSs. A simulation results have shown the effectiveness of the control system (Li et al. 2016).

An integral sliding mode observer for linear time variant systems is proposed by Jiménez-Rodríguez et al (Jiménez-Rodríguez et al. 2016). Second order sliding mode control is used to show the effectiveness of the controller. The simulation results demonstrated that the control system performed much better (Jiménez-Rodríguez et al. 2016).

The Backstepping Sliding Mode Control (BSMC) has been proposed by Coban (Coban 2017b). The BSMC is used to control the speed of the electromechanical system. The BSMC is compared with sliding mode control and backstepping control against the various parameter uncertainties. The BSMC has performed much better than the others (Coban 2017b).

A class of finite time control strategy is proposed by Chen et al (Chen, Du, and Jin 2017). A first order finite time control and an integral high order sliding mode control are designed. The simulation results are demonstrated that the controller outperformances at removing disturbance and about convergence (Chen, Du, and Jin 2017).

An extended state observer (ESO) based second order sliding-mode (SOSM) control for three-phase two-level grid-connected power converters are proposed by Liu et al (Liu et al. 2017). The noise occurred while using ESO and the gains of a super-twisting algorithm for the external control loop are removed without diminishing the settling time and decreasing the DC-link capacitor voltage drop. Experimental results have shown that the ESO SOSM controller gives much better performance than the conventional proportional integral synchronous reference frame control (Liu et al. 2017).

The Backstepping integral sliding mode control (BISMC) is designed for controlling the speed of an electromechanical system by Coban (Coban 2018) . An integral dynamic is added to sliding surface to remove chattering and to make the system performance better. The Lyapunov criterion is used to guarantee system stabilization. Experimental results of the BISMC and the SMC are given with graphs (Coban 2018).

The optimal H_∞ guaranteed cost sliding mode control problem for interval type-2 (IT2) fuzzy systems is concerned by Li et al (Li et al. 2018). A new integral sliding surface is proposed. The inverted pendulum system is used to show the effectiveness of the controller. The chattering is not fully removed (Li et al. 2018).

1.1. Contributions of This Thesis

Chattering phenomenon is the main problem while implementing the conventional SMC to the electromechanical system. In this thesis, the new dynamic integral switching function is proposed to remove the chattering effects with good robustness. The integral property is added to the switching function to build more durable system to parameter variations. For this purpose, the dynamic integral sliding mode control (DISMC) is applied to the electromechanical system to control speed by using a computer.

Unknown parameters and uncertainties diminish the electromechanical system performance. The proposed DISMC is utilized to overcome this deficiency due to its strong robustness. Hence, the DISMC is designed to show the robustness of the electromechanical system in existence of the parameter uncertainty. The various matched uncertainties to the system are examined. The conventional SMC and the DISMC are compared with various parameter uncertainties, because there is no comparison in the literature in this way (Coban 2017b).

The simulation and experimental results of this study are presented with graphs to make comparison of the conventional SMC and the DISMC. The simulation and experimental results of the conventional SMC and the DISMC are compared to demonstrate the power and effectiveness of the proposed controller. It is demonstrated in this study that the DISMC reduces chattering effect and increases the tracking accuracy.

1.2. Outline of This Thesis

The structure of the thesis is organized as follows:

Chapter 1: Introduction: In this chapter, the main information about the conventional SMC and the DISMC is explained. The previous works are researched and analyzed. The contributions of this thesis are described.

Chapter 2: Plant Description: Detailed mathematical model of the DC motor system is introduced in this chapter. The state space form and the linear form of the differential equations of the electromechanical system are given.

Chapter 3: Dynamic Integral Sliding Mode Control: In this chapter, the conventional sliding mode control is discussed and the dynamic integral sliding mode control is proposed. Lyapunov Stability Theorem is applied to the electromechanical system to guarantee the system stability. The electromechanical system is operated under various quantities of the parametric uncertainty. Saturation function is described for removing the chattering phenomenon.

Chapter 4: Simulation Results: A simulation program is coded to build the system structure and to calculate the system parameter approximately. The results of the conventional SMC and the DISMC with 20% and 80% parameter uncertainty are demonstrated with graphs and tables. In the end, the results of the conventional SMC and the DISMC are compared to show the effectiveness of the proposed controller.

Chapter 5: Experimental Results: The experimental servo set is explained in this chapter. The experimental results for the conventional SMC and the DISMC with and without parametric uncertainty are compared in terms of speed control, sliding surface and control signal. The graphs are presented to show the effectiveness of the proposed controller.

Chapter 6: Conclusions: Finally, conclusions are drawn in Chapter 6.

2. PLANT DESCRIPTION

2.1. DC Motor Model

DC motors are widely used in various industrial applications with their fast response, high efficiency, accurate, simple and continuous control characteristics. The DC motors are nonlinear systems since they have friction and dead-zone. The speed control of the DC motor precisely is necessary in many control implementations. A desired speed performance is reached when a desired shaft position is followed. If a linear model is intended to build and drive it with a linear control method, the control system does not give good tracking performance and regulation responses. Therefore, nonlinear control methods are more suitable to control the speed of the DC motors (Slotine and Li 1991a).

DC and AC motors are used in control systems but each has different features. DC servo motors are easy to control speed, position and have wide adjustable range. Hence, they are commonly used in various industrial applications (Horng 1999). Generally, a mathematical model of the DC servo motor is required to design of a controller.

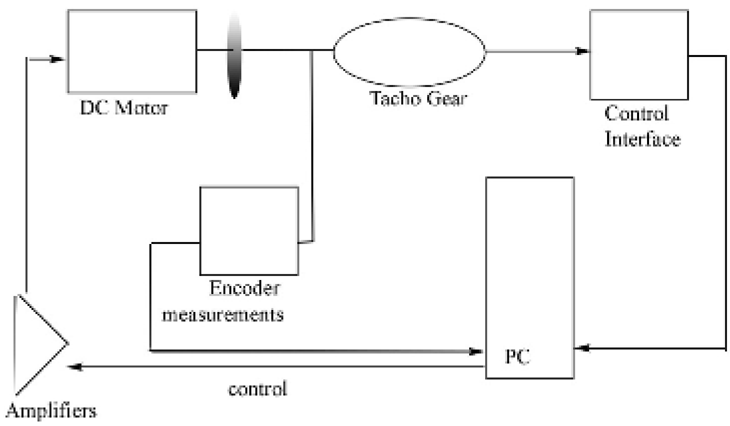

Figure. 0.1 The PMS Control System

In this study, an experimental setup that consists of a DC motor and some mechanical and electrical parts of it as shown in Fig.2.1 is used. A data acquisition card sends the input-output signals to the computer. The output speed is measured by a tachometer. The digital encoder computes the motor angular position. The digital data are carried to the I/O board. The correct signal range is supplied by pre-amplifier to the servo amplifier. The interface unit is exploited to proportion the analogue input and output to the I/O board in the computer to the true operating range. The input to motor control circuit is arranged by attenuator to the true operating level. Output potentiometer is used as a visual display of motor position. The electromechanical system under consideration operates at control input voltage in the range.

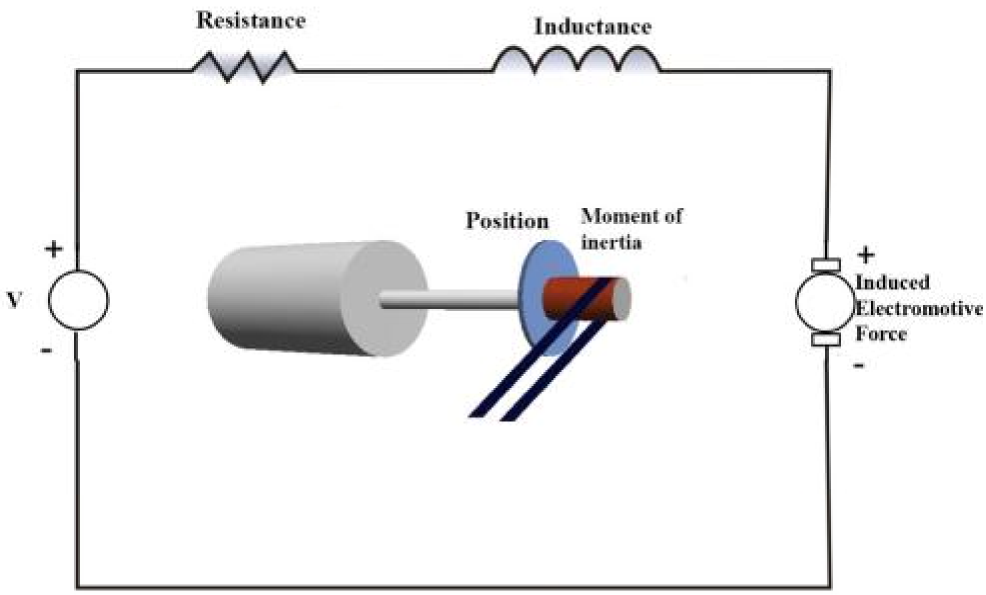

Figure. 0.2 DC Motor Model

The structure of the DC motor model is illustrated in Fig.2.2. The electrical and mechanical equations of the servo motor that is used in the laboratory can be given below

$$\tau(t) = K_t i(t) \tag{2.1}$$

where τ is torque; K_t is torque constant. The electromotive force, v_{emf}, is a voltage proportional to the angular shaft velocity $\dot{\theta}$:

$$v_{emf}(t) = \frac{K_b}{K_g}\dot{\theta}(t) \tag{2.2}$$

where K_b is a motor property dependent constant related to physical properties of the motor and K_g is the gain of the amplifiers. The mechanical dynamics can be described by using the Newton's law

$$J\ddot{\theta}(t) = \sum \tau_i(t) = -d\dot{\theta}(t) + K_t i(t) \tag{2.3}$$

where d is viscous friction; J is moment of inertia. The equations of the electrical model is

$$u(t) - v_{emf} = L\frac{di(t)}{dt} + Ri(t) \tag{2.4}$$

where R is resistance; L is inductance.
Substituting (2.2) into (2.4), the control signal $(u(t))$ is obtained:

$$u(t) = L\frac{di(t)}{dt} + Ri(t) + K_b\dot{\theta}(t). \tag{2.5}$$

The two main differential equations for the electromechanical system are constituted from (2.3) and (2.5):

$$\left.\begin{aligned}\frac{d^2\theta(t)}{dt^2} &= -\frac{\delta}{J}\dot{\theta}(t)+\frac{K_t}{J}i(t),\\ \frac{di(t)}{dt} &= -\frac{R}{L}i(t)-\frac{K_b}{L}\dot{\theta}(t)+\frac{1}{L}u(t)\end{aligned}\right\}. \tag{2.6}$$

The transformation of (2.6) into a vector-matrix form is stated below

$$\begin{aligned}\frac{d}{dt}\begin{bmatrix}\dot{\theta}(t)\\ i(t)\end{bmatrix} &= \begin{bmatrix}-\frac{\delta}{J} & \frac{K_t}{J}\\ -\frac{K_b}{L} & -\frac{R}{L}\end{bmatrix}\begin{bmatrix}\dot{\theta}(t)\\ i(t)\end{bmatrix}+\begin{bmatrix}0\\ \frac{1}{L}\end{bmatrix}u(t)\\ y(t) &= \begin{bmatrix}1 & 0\end{bmatrix}\begin{bmatrix}\dot{\theta}(t)\\ i(t)\end{bmatrix}\end{aligned} \tag{2.7}$$

where $y(t)$ is the output.

The equation (2.6) is transformed into the Laplace form as

$$s^2\theta(s) = -\frac{\delta}{J}s\theta(s)+\frac{K_t}{J}I(s) \tag{2.8}$$

and

$$sI(s) = -\frac{R}{L}I(s)-\frac{K_b}{L}s\theta(s)+\frac{1}{L}U(s)\ . \tag{2.9}$$

Substituting (2.9) into (2.8):

$$
\begin{aligned}
s^2\theta(s) &= -\frac{d}{J}s\theta(s)+\frac{K_t}{J}\left[-\frac{K_b}{sL+R}s\theta(s)+\frac{1}{sL+R}U(s)\right] \\
&= -\frac{d}{J}s\theta(s)-\frac{K_bK_t}{sLJ+RJ}s\theta(s)+\frac{K_t}{sLJ+RJ}U(s) \\
&= \frac{-(dLs+dR)-K_bK_t}{sLJ+RJ}s\theta(s)\frac{K_t}{sLJ+RJ}U(s)
\end{aligned}
\qquad (2.10)
$$

The equation (2.11) is obtained by rearranging (2.10):

$$
\begin{aligned}
s^3\theta(s) &= \frac{1}{LJ}\left[-RJs^2\theta(s)-dLs^2\theta(s)-dRs\theta(s)-K_bK_ts\theta(s)\right] \\
&\quad +\frac{K_t}{LJ}U(s).
\end{aligned}
\qquad (2.11)
$$

The equation (2.12) is formed by applying the inverse Laplace transformation to (2.11) and then including the additional gain K_g introduced by the amplifiers and converting the motor angular velocity from rad/s to rpm:

$$
\begin{aligned}
\dddot{\theta}(t) &= -\frac{R}{L}\ddot{\theta}(t)-\frac{d}{J}\ddot{\theta}(t)-\frac{dR}{LJ}\dot{\theta}(t)-\frac{K_bK_t}{LJ}\dot{\theta}(t)+\frac{K_gK_tT_{rpm}}{LJ}u(t) \\
&= \left(-\frac{R}{L}-\frac{d}{J}\right)\ddot{\theta}(t)-\left(\frac{dR+K_bK_t}{LJ}\right)\dot{\theta}(t)+\frac{K_gK_tT_{rpm}}{LJ}u(t)
\end{aligned}
\qquad (2.12)
$$

For notation simplification, $\omega(t)$ may be used instead of $\dot{\theta}(t)$, where $\omega(t)=\dot{\theta}(t)$. The following equation is obtained from (2.12) with this simplification:

$$
\ddot{\omega}(t) = \nabla(a\dot{\omega}(t) - b\omega(t)) + cu(t) \qquad (2.13)
$$

where $a = -\frac{R}{L} - \frac{d}{J}$, $b = \frac{dR + K_b K_t}{LJ}$, $c = \frac{K_g K_t T_{rpm}}{LJ}$, and ∇ is parameter uncertainties of the system.

While there are too much external disturbances, nonlinearity, and uncertainty in the real world systems, $d(t)$ is added to the plant (2.13):

$$\ddot{\omega}(t) = \nabla(a\dot{\omega}(t) - b\omega(t)) + cu(t) + d(t) \tag{2.14}$$

where $d(t)$ denotes the external disturbances, nonlinearity, and unmatched uncertainties. It is bounded but unknown, $|d(t)| < D$, where D is positive constant.

The DC motor parameters are given in Table 1. The other electromechanical system parameters determined experimentally are $J = 0.0001218 kgm^2, T_{rpm} = 60/(2\pi)$ and $d = 0.000425 Nms/rad$.

Table 2.1. Values of the electromechanical system parameters

Parameter		Value
K_t	torque constant	0.052 Nm / A
K_b	electromotive force constant	0.057 Vs/rad
R	resistance	2.5 Ω
L	inductance	0.0025 H
K_g	gain of the amplifiers	9.6

3. SLIDING MODE CONTROL

3.1. Introduction

Conventional sliding mode control (SMC), established at the early 1950s by Emelyanov, is the most powerful nonlinear variable structure control. This approach gives the system endurance against uncertainties when the conventional SMC is used to control the system (Vadim 1977; Sabanovic, Fridman, and Spurgeon 2004). The conventional SMC is suitable for uncertain nonlinear systems and the popularly used control method which provides high accuracy, robustness, fast response, good transient performance, order reduction and insensitivity to parameter variations against various internal and external perturbations (Chamsai, Jirawattana, and Radpukdee 2010), (Eker and Akınal 2008), (Slotine and Li 1991a). The conventional SMC has been widely used in industrial applications, that have DC servo motor systems, since it has superior properties (Perruquetti and Barbot 2002; Aydin and Coban 2016).

However, it has undesirable chattering effect on the sliding surface while implementing the conventional SMC for some real world applications (Iqbal, Bhatti, and Khan 2009; V. Utkin and Lee 2006; Jang, Chen, and Chen 2002). Chattering, which is created by the high frequency of switching, damages the property of the servo system and the actuators. The conventional SMC has been widely expanded to integrate new methods in order to overcome the chattering (Chamsai, Jirawattana, and Radpukdee 2010; Eker and Akınal 2008; Eker 2006; Shtessel and Shkolnikov 2003; Aksu and Coban 2016). One of them is the dynamic sliding mode control as it is more sturdy than the conventional SMC to overcome chattering against parameter variations (Tang and Zhang 2011; Eker and Akınal 2008). In this paper, a dynamic integral sliding mode control (DISMC) is proposed for this purpose.

The dynamic integral sliding mode control retains the principal advantages of the conventional SMC and furthermore, the performance of the DISMC is more accurate. Defining extra dynamics with integral action into the sliding surface helps to solve many difficulties in practice (Healey and Lienard 1993). The conventional SMC has been extended to the DISMC by adding an integral property to the sliding surface and extra dynamics. The DISMC is an augmented system that has the core idea of the dynamic sliding mode control (DSMC) and the integral sliding mode control and gives better results than the conventional SMC, the integral sliding mode, and the DSMC. Reaching phase is eliminated by integral sliding mode control and chattering is removed by DSMC as far as possible. It improves robustness and chattering reduction. Finally, the system is operated under parametric uncertainty to be a correct representation of some real systems, because there are more perturbations and disturbances while implementing in real world industrial applications (Coban 2017a). The results, which are taken from the DISMC under parametric uncertainty, are compared with those from the conventional SMC in dynamic responses.

The conventional sliding mode control method is widely used nonlinear control method recently. The conventional SMC is the strongest solution used in many practical applications with versatile use and simple design. It is based on the concept of altering the structure of the controller in reaction to alter the condition of the system to get the desired output. The advantages of the conventional SMC such as high accuracy, robustness, insensitivity to parameter variations and disturbances make the conventional SMC more preferred nonlinear control system (V. I. Utkin 1993b; Vadim 1977). System robustness means to be able to defeat adverse effects of uncertainties and disturbances.

The real world systems usually suffer from uncertainties. Hence, the sliding surface is used to solve this problem because the sliding surface converges to an equilibrium point in a finite time and varies randomly in the small area around it. Sliding surface plays an important role while designing the sliding mode controller because tracking error and output deviations could be kept at the satisfactory level. Defining a sliding surface is the most important step for designing a sliding mode controller (Fujisawa et al. 2004). The trajectories are pushed to lie on the sliding surfaces and maintain on there. If the plant trajectories are above the surface, a feedback has one gain and if the trajectory drops below the surface, it has different gain. The rule for proper switching is defined by the surface. This surface is also called a sliding surface (V. I. Utkin 1993a).

The switched control keeps the state trajectory on the surface forever and the state of the system slides on the surface toward the stable equilibrium point. The most important part is to design a switched control that drives the system state to the switching surface and hold it on the surface once intercepted. A Lyapunov approach is used to accomplish this task.

Stability theory has a great important effect on the engineering, especially in the control theory and automation. Stability provides qualitative results about system performance. Dynamic system stability has essential requirement of real world problems and practical applications. In general, stability means that the system outputs and inputs are limited with acceptable bounds or the system outputs meet around an equilibrium point (the asymptotical stability). The output may have oscillation behavior. If the oscillation maintains its existence or raise the magnitude, the system will be unstable. On the other hand, if the oscillation diminishes the magnitude, the closed loop system will be stable.

There are too many types of stabilities, however taking the basic points that divided them into three parts: the equilibrium stability, the orbital stability and the structural stability. The Lyapunov stability is used in this thesis, since its ideas and techniques are pioneering to basic stability research and applications.

Stability theory plays a pivotal role in control theory. There are various types of control stability for the solution of differential equations defining dynamical systems. In this thesis, Lyapunov stability theorem which is stability of equilibrium points is used. Lyapunov stability is named Aleksandr Lyapunov, a Russian mathematician and engineer who construct the foundation of the theory. An equilibrium point is stable if all solutions starting at nearby points stay nearby; on the other hand, it is unstable.

Theorem 3.3. The Lyapunov Stability Theorem:

a) The system is stable if for every $t \geq 0$ there exists $V(t) > 0$ and $V(0) = 0$ such that for each t with $\dot{V}(t) \leq 0$.
b) The system is unstable if it is not stable.
c) The system is asymptotically stable if for every $t \geq 0$ there exists $V(t) > 0$ and $V(0) = 0$ such that for each t with $\dot{V}(t) < 0$ (Slotine and Li 1991b).

Lyapunov stability theorem is applied to the system to design the sliding mode controller. A candidate Lyapunov function, that characterizes the motion of the system state to the sliding surface, is defined. For each chosen switched control structure, the "gains" are chosen such that the derivative of the Lyapunov stability function is negative definite, thus ensuring motion of the system state to the surface. After appropriate design of the sliding surface, a switched controller is designed so that the system state trajectories point towards the surface such that the state is driven to the this surface. Once system states reach to the sliding surface, they remain on it. This kind of controllers results in discontinuous closed-loop systems.

3.2. Chattering Phenomenon

The chattering phenomenon is usually defined as a motion that oscillates around a sliding surface. The chattering phenomenon is the main obstacle to the success of these techniques in the real world systems. Actually, ideal sliding mode doesn't have the chattering phenomenon, but all of the sliding mode control, that is used in the real world, doesn't have to be ideal. Therefore, the point reaches the sliding surface and has a velocity and pass it, passing it means the sign of the switching condition changes, so the structure of the controller would change immediately. But this action is not finished instantly. In this way, chattering appears as shown in Fig.3.1.

There are many factors that contribute to the chattering phenomenon, so different approaches are put forward to reduce the chattering in the

In practice, depending on the end sampling time used, the system state does not slide directly on the sliding surface. Instead, the sampling frequency is chattering with the same frequency in the sliding surface. The unmodelled chattering in high order dynamics is not desirable situation (V. Utkin and Lee 2006).

The saturation function is used instead of signum function to prevent the system from chattering phenomenon (Vadim Utkin, Guldner, and Shi 2009).

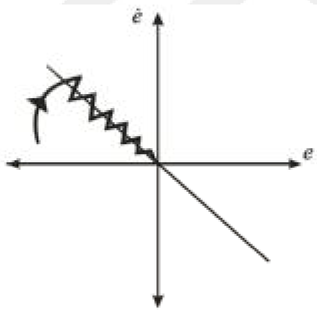

Figure. 0.1 Chattering Phenomenon in Sliding Mode Control

The saturation function, which is demonstrated in Fig.3.2, is adopted in the following equation

$$sat(s(t)) = \begin{cases} 1, & s(t) > \phi \\ ks(t), & |s(t)| \le \phi \;,\; k = 1/\phi \\ -1, & s(t) < -\phi \end{cases} \tag{3.21}$$

where f is called boundary layer; s(t) is sliding surface. The feedback control is used inside the boundary layer and the switch control is used outside the boundary layer. Hence, the chattering phenomenon is reduced effectively.

The advantage of using the saturation function in the system is that a boundary layer is added around the sliding surface. In the boundary layer, neither intense switching nor chattering occurs in the control action (V. Utkin and Lee 2006).

However, it cannot guarantee that the sliding state, defined by Lyapunov function in the equation, can be realized.

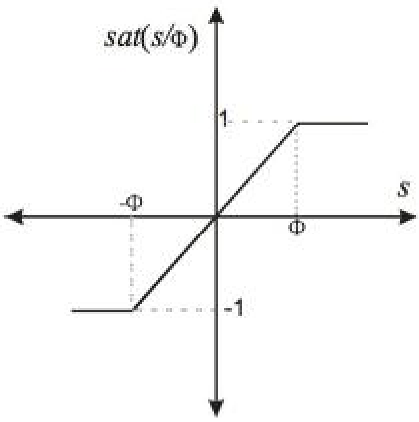

Figure. 0.2 Saturation Function

3.3. Types of the SMC

3.3.1. Conventional Sliding Mode Control

There are two steps which must have been done while constructing the conventional sliding mode control. Designing a sliding surface is the first step, and the second one is to construct the switched feedback gains necessary to drive the system state trajectory to the sliding surface. The block diagram of the conventional SMC is demonstrated in Fig.3.3.

The tracking error, that is the difference between the set-point $\left(w_r(t)\right)$ and the output $\left(w(t)\right)$, is given by

$$e(t) = \omega_r(t) - \omega(t). \tag{3.1}$$

Sliding surface $(s(t))$ is connected with the tracking error $(e(t))$ and the derivatives of it as

$$s(t) = \left(\sum_{i=1}^{n-1} c_i + \frac{d}{dt} \right)^{n-1} e(t) \tag{3.2}$$

where n implies order of the nonlinear system, and $c_i \in \mathbb{R}^+$.

The system used in this paper is of second order, so $n = 2$. The equation (3.2) can be rewritten as follow

$$s(t) = c_1 e(t) + \dot{e}(t) \tag{3.3}$$

where c_1 must satisfy Hurwitz condition, $c_1 \in \mathbb{R}^+$.

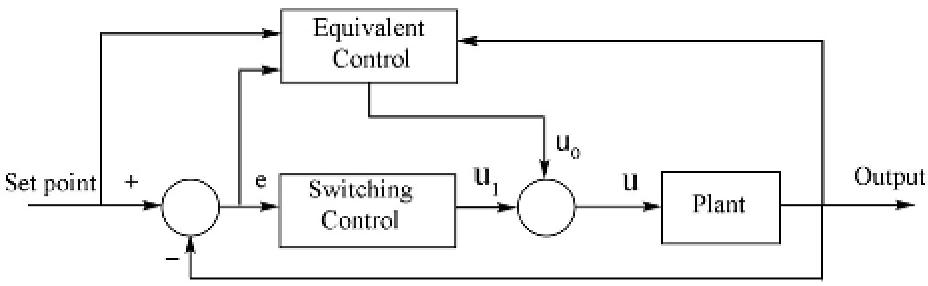

Figure. 0.3 Conventional Sliding Mode Control

Pushing the tracking error $(e(t))$ to carry on the sliding surface $(s(t))$ and then go on the sliding surface to the origin is the aim of the conventional sliding mode control. The tracking error $(e(t))$ should converge to zero in a finite time for guaranteeing stabilization of the sliding surface $(s(t))$, that is $\lim_{t \to \infty} e(t) = 0$. This means that the system is going to follow the desired trajectory asymptotically.

There are two phases of the conventional sliding mode control, the sliding phase with $s(t) = 0$, $\dot{s}(t) = 0$ and the reaching phase $s(t) \neq 0$.

When the system is in the sliding phase, both $s(t) = 0$ and $\dot{s}(t) = 0$. Taking derivatives of (3.3) results in

$$\dot{s}(t) = c_1 \dot{e}(t) + \ddot{e}(t) = 0. \tag{3.4}$$

Substituting $\ddot{e}(t) = \ddot{w}_r(t) - \ddot{w}(t)$ and (2.14) into (3.4), then the following equation is obtained:

$$\dot{s}(t) = c_1 \dot{e}(t) + \ddot{w}_r(t) - \left[-a\dot{w}(t) - bw(t) \right] - cu(t) - d(t) = 0. \tag{3.5}$$

Since the conventional sliding mode controller $(u(t))$ consists of the equivalent control $(u_0(\mathrm{t}))$ and the switching control $(u_1(\mathrm{t}))$, it can be defined as follows:

$$u(t) = u_0(t) + u_1(t) \quad . \tag{3.6}$$

The equivalent control $(u_0(\mathrm{t}))$ makes the state trajectory stay on the sliding surface while the system is pushed by the switching control to slide on the sliding surface.

The equivalent control u_0(t) is solved for $u(t)$ in (3.5) when d(t) is ignored :

$$u_0(t)=\frac{1}{c}\left(c_1\dot{e}(t)+\ddot{\omega}_r(t)-\nabla\left[a\dot{\omega}(t)-b\omega(t)\right]\right). \qquad (3.7)$$

The switching control $\left(u_1\text{(t)}\right)$ must be selected to meet the reaching condition aspects. It should force the system states to the sliding surface. The switching control $\left(u_1\text{(t)}\right)$ is selected in the literature as

$$u_1(t)=\eta\, sat(s(t)) \qquad (3.8)$$

where $\eta > 0$, that should be chosen as large as needed to remove all uncertainties, and $sat(.)$, demonstrated in Fig.3.2., indicates the saturation function for removing chattering described as

$$sat(s(t))=\begin{cases}\operatorname{sgn}(s(t)), & |s(t)|>\phi\\ ks(t), & |s(t)|\le\phi\end{cases}\quad,\quad k=1/\phi \qquad (3.9)$$

.

The conventional sliding mode controller $\left(u(t)\right)$ is obtained, when (3.7) and (3.8) is substituted into (3.6).

The Lyapunov function candidate may be selected as

$$V(t) = \frac{1}{2}s^2(t) \tag{3.11}$$

where $V(t)$ is the Lyapunov function, $V(0) = 0$ and $V(t)$ is positive definite function $(V(t) > 0)$, for $t > 0$ where $s(t) \neq 0$. Derivative of V(t) in (3.11) must be negative definite $(\dot{V}(t) < 0)$:

$$\dot{V}(t) = s(t)\dot{s}(t) < 0, \quad s(t) \neq 0. \tag{3.12}$$

Theorem 3.3.1: *The closed-loop system consisting of the plant (2.14) and the conventional sliding mode controller (3.10) has a globally asymptotically stable at* $(e(t) = 0)$ *and* $\lim_{t \to \infty}(\omega_r(t) - \omega(t)) = 0$ *in the presence that the disturbance is bounded.*

Proof: Firstly, for every $t \geq 0$, $V(0) = \frac{1}{2}s^2(0) = 0$.

Then, for every $t \geq 0$, $V(t) = \frac{1}{2}s^2(t) > 0$.

When the first derivative of Lyapunov function (3.11) with respect to time is taken, it is less than zero as given below:

$$\begin{aligned}\dot{V}(s(t)) &= s(t)\dot{s}(t)\\ &= s(t)\Big[c_1\dot{e}(t)+\ddot{\omega}_r(t)-\nabla\left(a\dot{\omega}(t)-b\omega(t)\right)\\ &\quad -c\left(u_0(t)+u_1(t)\right)-d(t)\Big]\end{aligned} \tag{3.13}$$

Substituting (3.7) into (3.13), one has

$$\begin{aligned}\dot{V}(s(t)) &= s(t)\left(-u_1(t)+d(t)\right)\\ &\le -\eta\, s(t)sat(s(t))\\ &= -\eta\,|s(t)|<0\end{aligned} \tag{3.14}$$

with the switching function (3.8) where $\eta > D$.

The first derivative of the Lyapunov function is negative $(\dot{V}(t)<0)$. Then, the system is asymptotically stable. The conventional sliding mode control system stability is guaranteed with the Lyapunov Stability Theorem. □

3.3.2. Dynamic Integral Sliding Mode Control

The Dynamic Integral Sliding Mode Control (DISMC) keeps the advantages of the integral sliding mode control and dynamic sliding mode control. The sliding mode is constructed without reaching phase for the integral sliding mode control. Unfortunately, there is a frequently encountered problem which is called chattering in the implementation of the conventional SMC. The dynamic integral sliding mode control overcomes the chattering sufficiently, eliminates the reaching phase and inherits all advantages of the conventional SMC (Koshkouei, Burnham, and Zinober 2005). The DISMC is designed by adding integral property to sliding surface and yielding chatter free control with the desired performance. It is robust control method with respect to parameter variations and imprecisions (Xue and Li 2016).

The dynamic with integral augmented sliding surface is

$$s(t) = c_1 e(t) + \dot{e}(t) + c_2 \int_0^t e(\tau)\, d\tau \tag{3.15}$$

where c_1 is the positive constant, c_2 is the integral gain and $c_1, c_2 > 0$. Taking the derivative of the equation (3.15) yields

$$\dot{s}(t) = c_1 \dot{e}(t) + \ddot{e}(t) + c_2 e(t) \tag{3.16}$$

and substituting $\ddot{e} = \ddot{\omega}_r(t) - \ddot{\omega}(t)$ and (2.14) into (3.16), one has

$$\dot{s}(t) = \nabla\left(a\dot{\omega}(t) - b\omega(t)\right) + cu(t) + d(t) + c_1 \dot{e}(t) + c_2 e(t) + \ddot{\omega}_r(t). \tag{3.17}$$

New dynamic sliding surface is defined as

$$\sigma(t) = \dot{s}(t) + \lambda s(t) \tag{3.18}$$

where λ must satisfy the Hurwitz condition, hence $\lambda > 0$.

The new dynamic sliding surface (3.18) is asymptotically stable, if those cases are satisfied:

I. $\sigma(t) = 0$,

II. $e(t) \to 0$,

III. $\dot{e}(t) \to 0$.

The new dynamic sliding surface can be rearranged substituting (3.17) into (3.18):

$$\begin{aligned}\sigma(t) &= \dot{s}(t) + \lambda s(t) \\ &= \nabla\left(a\dot{\omega}(t) - b\omega(t)\right) + cu(t) + \dot{d}(t) \\ &\quad + \ddot{\omega}_r(t) + c_1\dot{e}(t) + c_2 e(t) + \lambda s(t).\end{aligned} \tag{3.19}$$

The derivative of the new dynamic sliding surface (3.19) with respect to time is given below:

$$\begin{aligned}\dot{\sigma}(t) &= \nabla\left(a\ddot{\omega}(t) - b\dot{\omega}(t)\right) + c\dot{u}(t) + \ddot{d}(t) \\ &\quad - \dddot{\omega}_r(t) + c_1\ddot{e}(t) + c_2\dot{e}(t) + \lambda\dot{s}(t).\end{aligned} \tag{3.20}$$

Substituting $\ddot{e}(t) = \ddot{\omega}_r(t) - \ddot{\omega}(t)$ and (3.17) into (3.20), the derivative of the new dynamic sliding surface can be rewritten as

$$\begin{aligned}\dot{\sigma}(\mathrm{t}) &= -\left(\nabla a + c_1 + \lambda\right)\ddot{\omega}(t) - \nabla b\dot{\omega}(t) + (c_1 + \lambda)\ddot{\omega}_r(t) + \dddot{\omega}_r(t) \\ &\quad - c\dot{u}(t) + \lambda c_2 e(t) + \left(\lambda c_1 + c_2\right)\dot{e}(t) - \ddot{d}(t).\end{aligned} \tag{3.21}$$

he dynamic equivalent controller is selected from (3.21) by setting the time derivative of the new dynamic sliding surface to zero when $d(t)$ is ignored:

$$\begin{aligned}\dot{u}_0(t) = \frac{1}{c}\Big[&\left(\nabla a + c_1 + \lambda\right)\ddot{\omega}(t) + \nabla b\dot{\omega}(t) - (c_1 + \lambda)\ddot{\omega}_r(t) \\ &- \dddot{\omega}_r(t) - \lambda c_2 e(t) - \left(\lambda c_1 + c_2\right)\dot{e}(t)\Big].\end{aligned} \tag{3.22}$$

The discontinuous law:

$$u_1(t) = -\eta \,\mathrm{sgn}(\sigma(t)) \tag{3.23}$$

Since the DISMC $\left(u_{DISMC}(t)\right)$ consists of the equivalent control $\left(u_0(\mathrm{t})\right)$ and the switching control $\left(u_1(\mathrm{t})\right)$, it can be defined as follows:

$$\begin{aligned} u_{DISMC}(t) &= u_0(t) + u_1(t) \\ &= \frac{1}{c}\Big[\left(\nabla a + c_1 + \lambda\right)\dot{\omega}(t) + \nabla b\,\omega(t) - \left(c_1 + \lambda\right)\dot{\omega}_r(t) \\ &\quad - \ddot{\omega}_r(t) - \lambda c_2 e(t) - \left(\lambda c_1 + c_2\right)\dot{e}(t)\Big] - \eta\,\mathrm{sgn}(\sigma(t)) \end{aligned} \tag{3.24}$$

Theorem 3.3.2: *The closed-loop system consisting of the plant (2.14) and the dynamic integral sliding mode controller (3.24) has a globally asymptotically stable at* $\left(e(t) = 0\right)$ *and* $\lim_{t \to \infty}(\omega_r(t) - \omega(t)) = 0$ *in the presence that the disturbance is bounded.*

Proof: Firstly, for every $t \geq 0$, $V(0) = \frac{1}{2}s^2(0) = 0$.

Then, for every $t \geq 0$, $V(t) = \frac{1}{2}s^2(t) > 0$.

When the first derivative of the Lyapunov function (3.11) with respect to time is taken, it is less than zero.

$$\begin{aligned}\dot{V}(\sigma(t)) &= \sigma(t)\dot{\sigma}(t) \\ &= \sigma(t)\Big[-\left(\nabla a + c_1 + \lambda\right)\ddot{\omega}(t) - \nabla b\dot{\omega}(t) + (c_1+\lambda)\ddot{\omega}_r(t) \\ &\quad + \dddot{\omega}_r(t) - c\dot{u}(t) + \lambda c_2 e(t) + \left(\lambda c_1 + c_2\right)\dot{e}(t) - \dot{d}(t)\Big].\end{aligned} \tag{3.25}$$

Substituting derivative of (3.24) into (3.23) for $\dot{u}(t)$, one has

$$\begin{aligned}\dot{V}(\sigma(t)) &= \sigma(t)\dot{\sigma}(t) \\ &= \sigma(t)\Big[-\left(\nabla a + c_1 + \lambda\right)\ddot{\omega}(t) - \nabla b\dot{\omega}(t) + (c_1+\lambda)\ddot{\omega}_r(t) \\ &\quad + \dddot{\omega}_r(t) - c\dot{u}(t) + \lambda c_2 e(t) + \left(\lambda c_1 + c_2\right)\dot{e}(t) - \dot{d}(t)\Big] \\ &= -\eta\sigma(t)\operatorname{sgn}(\sigma(t)) \\ &\leq -\eta\left|\sigma(t)\right| \\ &< 0.\end{aligned} \tag{3.26}$$

where $\eta > 0$,$\eta > D$ and that η should be chosen as large as needed to remove all uncertainties and disturbances.

The first derivative of (3.13) with respect to time is negative definite according to (3.26). Therefore, the DISMC system (3.24) is globally asymptotically stable. The dynamic integral sliding mode control system stability is guaranteed with the Lyapunov Stability Theorem. □

4. SIMULATION RESULTS

In this section, numerical results are obtained with a simulation program using the conventional sliding mode controller and the dynamic integral sliding mode controller. The equation (2.14) is used as a plant under parameter uncertainty to control the speed of the electromechanical system.

The nonlinear control system controlled by the conventional SMC and the DISMC is coded in a simulation program. A step function is selected for the input signal. The controller controls the system based on the tracking errors values generated.

In this situation, no matched uncertainty $(\nabla = 1)$ is taken for the electromechanical system (2.14). The graphs of sliding surface, control input and speed of the system are plotted for the conventional SMC and the DISMC. Heuristic method is generally used to select the sliding mode controller parameters. There are a few things to be considered in here. All the parameters of the sliding mode control must be positive. The overshoot is not desired. The parameters of the new dynamic sliding surface (3.19) must be stable. From all of these, the parameters are chosen to satisfy the requirements to be $c_1 = 100,\ c_2 = 100,\ \lambda = 40,\ \eta = 2 \times 10^9$. A step reference trajectory of 1600 rpm is applied to the control systems for all experiments. The sampling period is taken 2 seconds for all conditions.

The tracking responses of the conventional SMC and the DISMC to a step reference 1600 rpm are illustrated in Fig.4.1.a. The performance of the system with the DISMC is much better than the performance with the conventional SMC. The rise time and the settling time of the DISMC are also better. The settling time for the DISMC and the conventional SMC is approximately 0.085 s and 0.6 s, respectively. No overshoot and no chattering are observed for the conventional SMC and the DISMC.

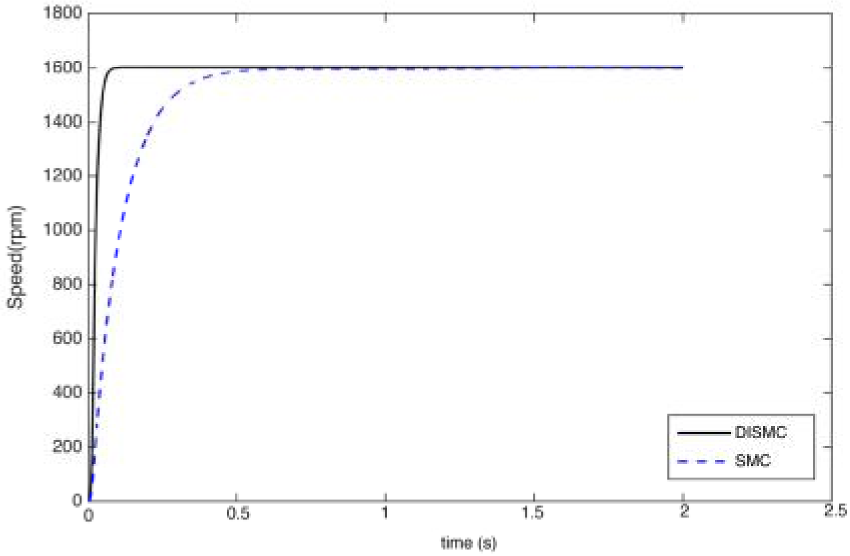
1800
1600
1400
1200
1000
800
600
400
200
0
Speed(rpm)
0
0.5
1
1.5
2
2.5
time (s)
DISMC
SMC

(a)

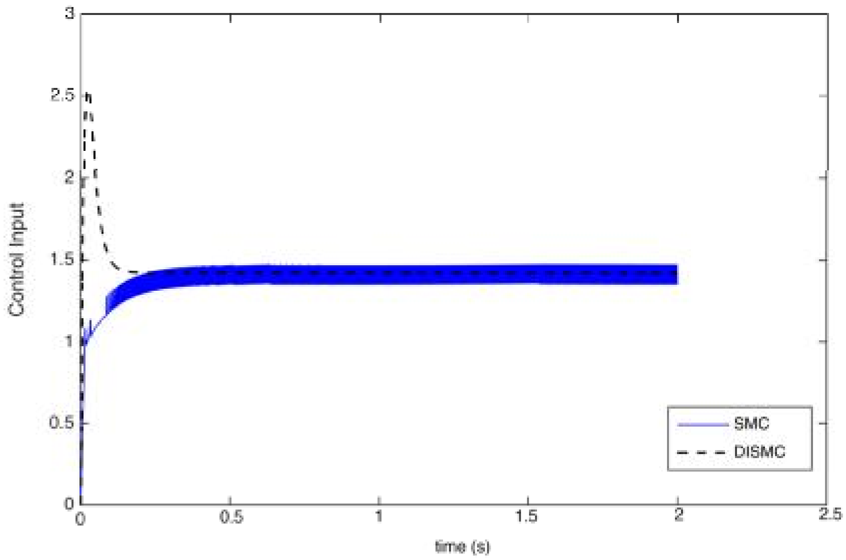
3
2.5
2
1.5
1
0.5
0
Control Input
0
0.5
1
1.5
2
2.5
time (s)
SMC
DISMC

(b)

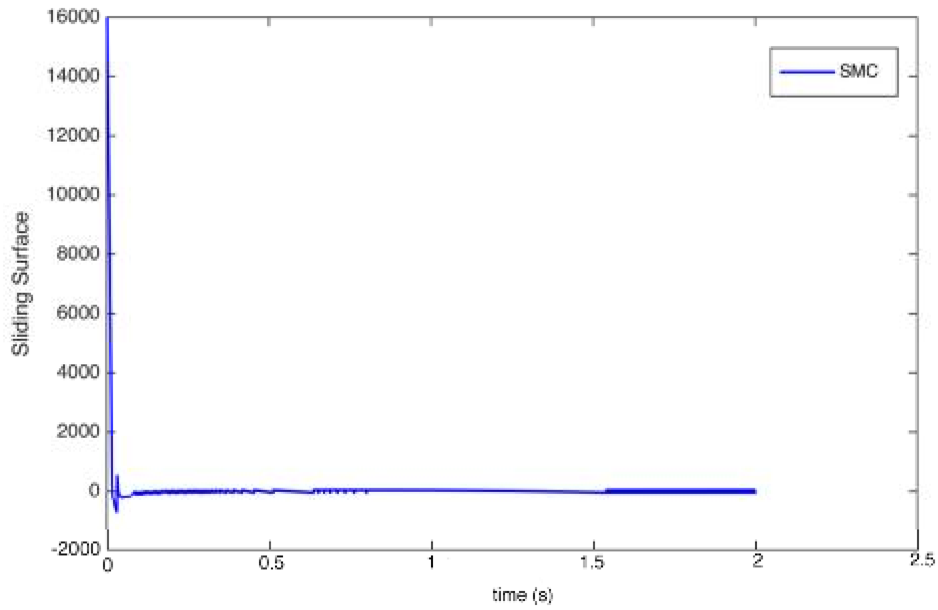

16000
14000
12000
10000
8000
6000
4000
2000
0
-2000
Sliding Surface
SMC
0
0.5
1
1.5
2
2.5
time (s)

(c)

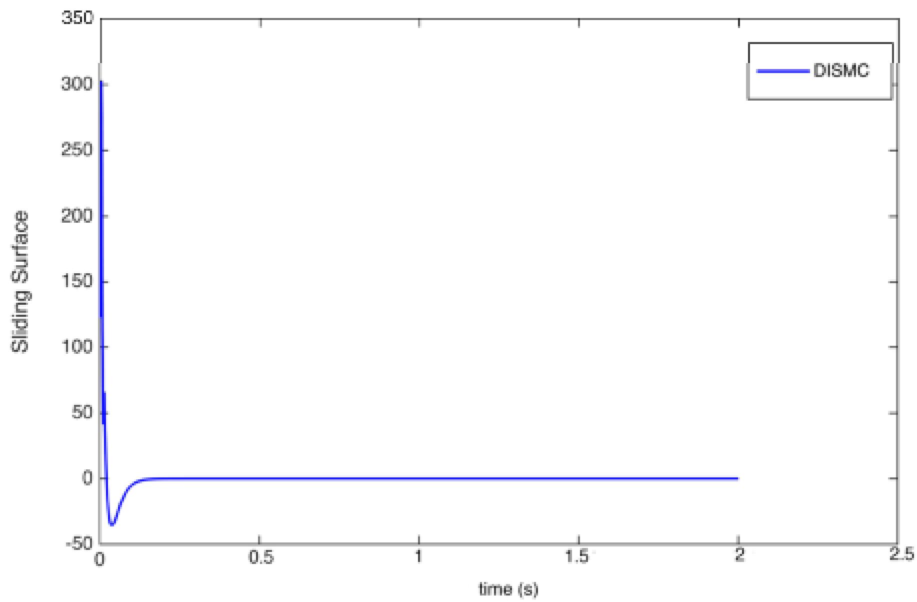

350
300
250
200
150
100
50
0
-50
Sliding Surface
DISMC
0
0.5
1
1.5
2
2.5
time (s)

(d)

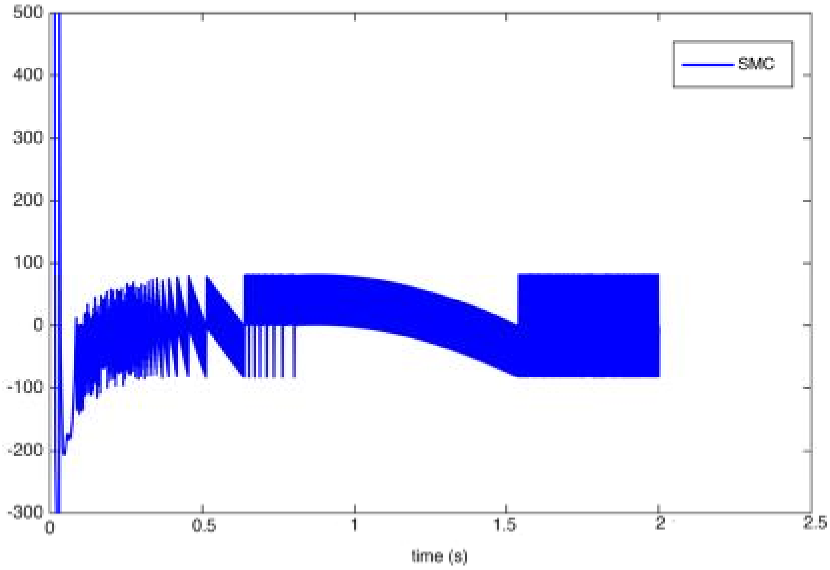

(e)

Figure. 0.1. Simulation Results for no uncertainty $\tilde{N} = 1$: (a) Tracking Responses of the conventional SMC and the DISMC, (b) Control Inputs of the conventional SMC and the DISMC, (c) Sliding Surface of the conventional SMC, (d) Sliding Surface of the DISMC, (e) Magnified version of the Sliding Surface of the Graph 4.1.c.

The control input signals for the conventional SMC and the DISMC are showed in Fig. 4.1.b. The control input for the DISMC has no chattering; on the other hand the control input for the conventional SMC has chattering. The DISMC converges at 0.2 s and the conventional SMC converges at 0.4 s. Moreover, the input signals of two controllers stay with in its bound of |2.5| V. Hence, the DISMC gives faster response than the conventional SMC.

The variations of the sliding surfaces during the control for the conventional SMC and the DISMC are illustrated in Fig.4.1.c. and Fig.4.1.d. It is remarkable to say that the sliding function is $s(t) \neq 0$ when the error signal is not zero. The sliding signal reaches to the sliding surface for the conventional SMC and the DISMC 0.1 s. However, the deviations and fluctuations of the conventional

SMC are much more. They occur because of the uncertainties, the errors and the disturbances. The Fig.4.1.e. is the magnified version of the Fig.4.1.c. The Fig.4.1.e is given to show the differences between the conventional SMC and the DISMC because the boundary of y-axis in Fig.4.1.c is different from the Fig.4.1.d. It is clearly inferenced from the Fig.4.1.c. and the Fig.4.1.d. that the deviations and fluctuations of the variations are smaller in the DISMC control than the conventional SMC.

In this situation, the parametric uncertainty is introduced into the electromechanical system with 20 percent variations of the actual parameters $(\nabla = 0.8)$. The parameters are chosen to satisfy the requirements to be $c_1 = 100,\ c_2 = 100,\ \lambda = 35,\ \eta = 3 \times 10^9$. The conventional SMC and the proposed control method (the DISMC) are applied to the electromechanical system under this parameter uncertainty. The robustness of the conventional SMC and the DISMC are compared against the parameter uncertainty.

The speed responses of the system are shown in Fig.4.2.a. for the conventional SMC and the DISMC. The output speed of the DISMC settles down at 0.15 s and the output speed of the conventional SMC settles down at 0.2 s in Fig.4.2.a. The system speed with the proposed controller (DISMC) is faster than those with the conventional SMC. The conventional SMC exhibit steady-state error about 30 rpm, but there is no steady-state error for the DISMC. The conventional SMC has chattering effect, but the DISMC has no chattering. There is no overshoot for two controllers. The DISMC diminishes the reaching phase, has smaller raising time. The DISMC outperforms the conventional SMC at reducing chattering under the parameter uncertainty. The performance of the DISMC is much better than the conventional SMC. There is better rising time, has no overshoot and no chattering for DISMC.

The control efforts are illustrated in Fig.4.2.b for the conventional SMC and the DISMC. The conventional SMC displays oscillations with great magnitude in the presence of parametric variation. These oscillations aren't as hazardous as chattering for the system, but still harm the actuators. The DISMC control effort is smooth, has no oscillations and decreases the chattering by comparison with the conventional SMC.

The sliding manifolds (surfaces) for the conventional SMC and the DISMC are shown in Fig.4.2.c. The conventional SMC sliding surface converges to the origin with chattering, but the DISMC sliding surface converges almost without any chattering. The settling time is almost eliminated with the DISMC. There is an overshoot for the conventional SMC, but not for the DISMC. The sliding signal reaches to the sliding surface for the conventional SMC and the DISMC; however the deviation and the fluctations of the conventional SMC are much more than the DISMC.

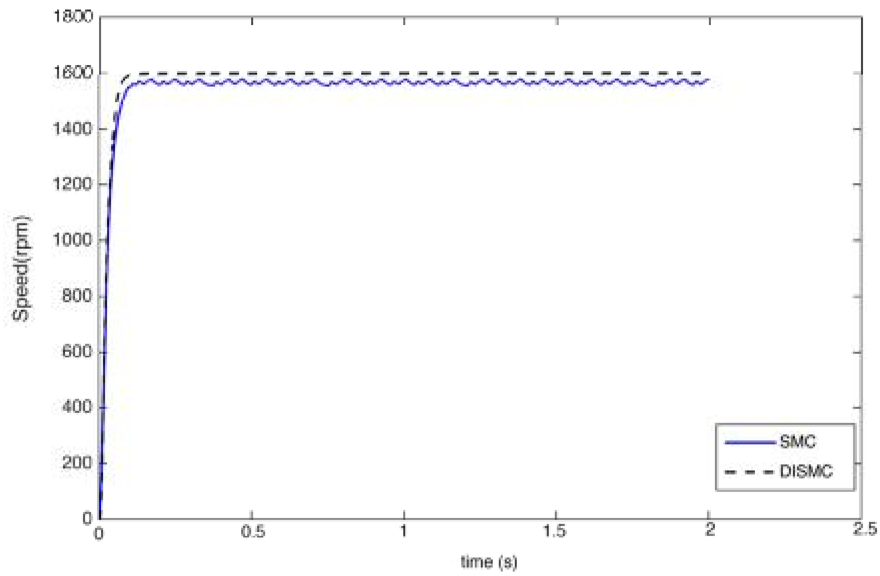

(a)

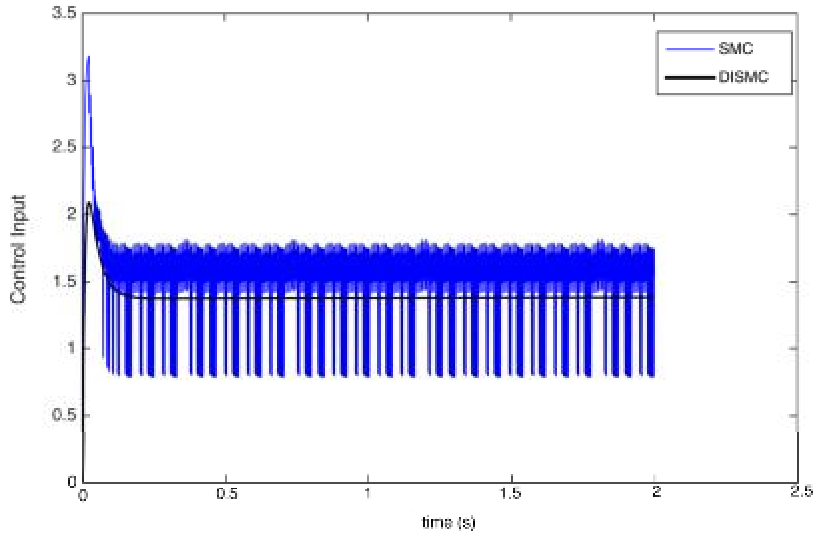

(b)

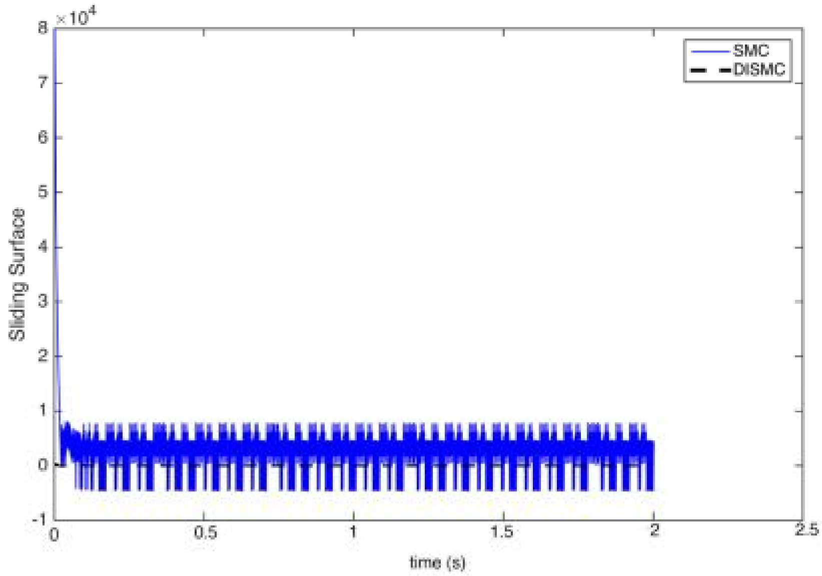

(c)

Figure. 0.2. Simulation Results for uncertainty $\tilde{N} = 0.8$: (a) Tracking Responses of the conventional SMC and the DISMC, (b) Control Inputs of the conventional SMC and the DISMC, (c) Sliding Surfaces of the conventional SMC and the DISMC.

This last simulation with 80% of match uncertainty is done to make more certain remarks on robustness of the DISMC and the conventional SMC $(\nabla = 0.2)$. The parameters are chosen for this simulation to meet the conditions as $c_1 = 140,\ c_2 = 600,\ \lambda = 65,\ \eta = 8 \times 10^9$. The difference between performances of the controllers is increased in this situation.

The speed responses of the system are shown in Fig.4.3.a. for the conventional SMC and the DISMC. The output speed of the DISMC settles down at 0.1 s and the output speed of the conventional SMC settles down at 0.2 s in Fig.4.3.a. The system speed with the proposed controller (DISMC) responds faster than those with the conventional SMC. The conventional SMC exhibits steady-state error about 40 rpm, but there is no steady-state error for the DISMC. The conventional SMC has chattering effect, but the DISMC has no chattering. There is no overshoot for the conventional SMC and the DISMC. The DISMC diminishes the reaching phase, has smaller raising time. The DISMC outperforms the conventional SMC at reducing chattering under the parameter uncertainty. The performance of the DISMC is much better than the conventional SMC. There is better rising time, has no overshoot and no chattering for the DISMC.

The control efforts are illustrated for the conventional SMC and the DISMC in Fig.4.3.b. The conventional SMC displays oscillations with great magnitude in the presence of parametric variation. The DISMC control effort has also oscillations, but not as much as the conventional SMC and decreases the chattering by comparison with the conventional SMC.

The sliding manifolds for the conventional SMC and the DISMC are shown in Fig.4.3.c. The conventional SMC sliding surface converges to the origin with great magnitude oscillations, but the DISMC sliding surface converges exactly without any oscillations. The settling time is almost eliminated with the DISMC. There is no overshoot for the DISMC. The sliding signal reaches to the sliding surface for only the DISMC; however the deviations and the fluctations of the conventional SMC are much more than the DISMC.

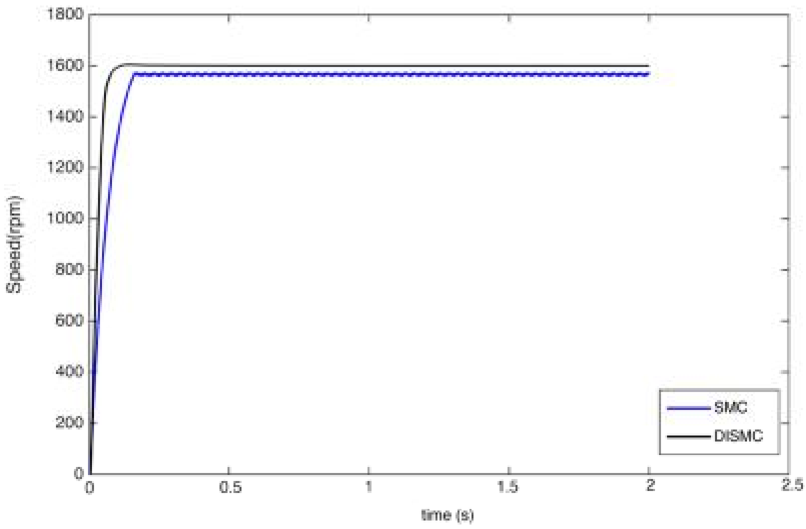

(a)

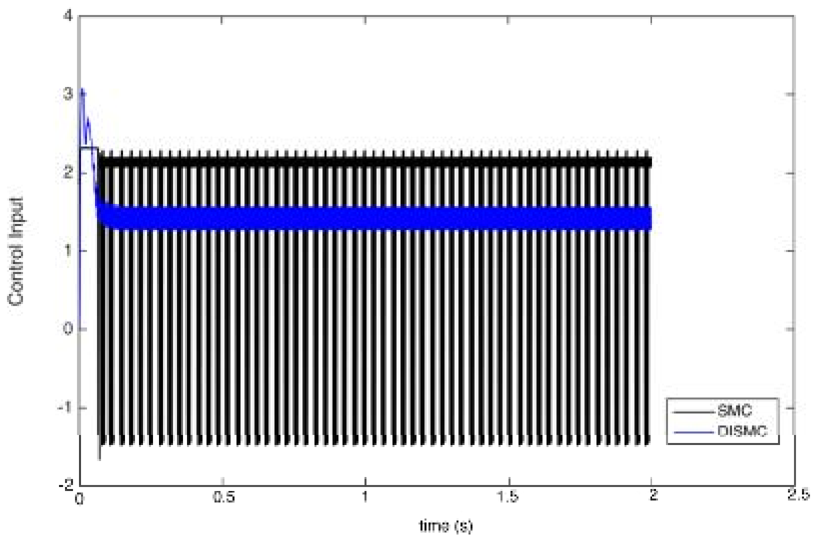

(b)

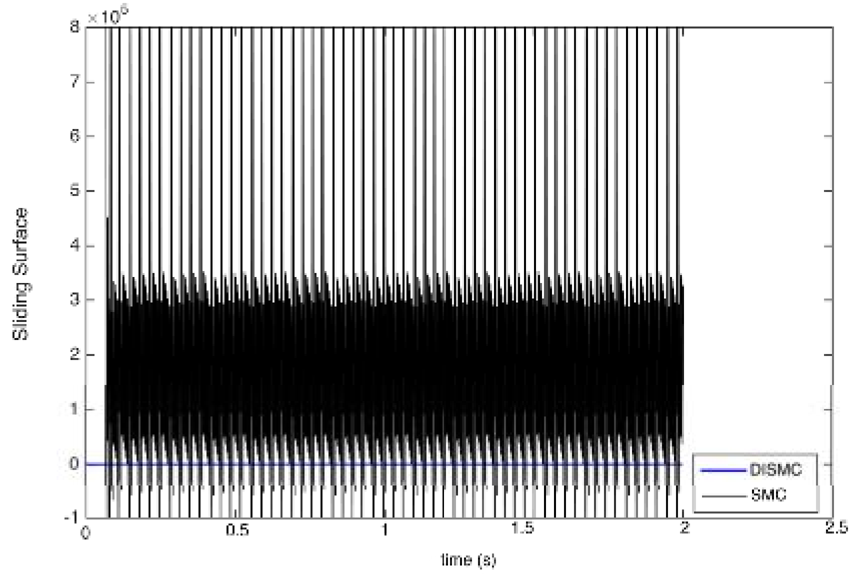

(c)

Figure. 0.3. Simulation Results for uncertainty $Ñ = 0.2$: (a) The Output Speeds of the conventional SMC and the DISMC, (b) Control Inputs of the conventional SMC and the DISMC, (c) Sliding Surfaces of the conventional SMC and the DISMC.

The DISMC is more robust than the conventional SMC under parametric uncertainties. The DISMC has not only fast response but also more robust than the conventional SMC. The DISMC is more preferable for electromechanical systems in many control applications, because the conventional SMC may damage actuators in the systems.

5. EXPERIMENTAL RESULTS

A diagram of experimental setup is depicted in Fig.5.1. An experiment servo set is used to implement the conventional SMC and the proposed DISMC as shown in Fig.5.2. The Precision Modular Servo set mechanical unit is composed of a DC Motor, Input Output Potentiometers, Tachometer, Magnetic Brake and Digital Encoder. The measured signals are allowed to be transferred into the computer by a data acquisition card.

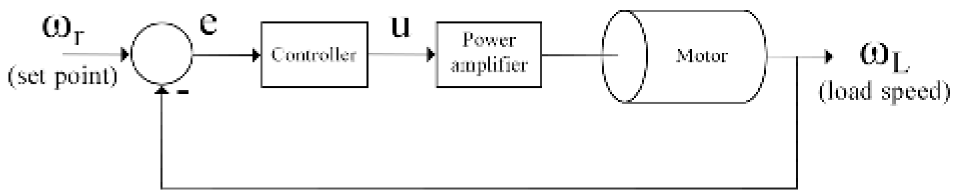

Figure. 0.1. Block Diagram of the Control System

The DC servo motor that is a 24V DC brushed motor with a no-load speed of 4050 rpm is used. The sampling period is taken 2 ms for all conditions. The experimental application is tested by using a program environment.

For the beginning, the conventional SMC and the proposed control method (DISMC) are applied to the electromechanical system under various parameter uncertainties. The parametric uncertainty is introduced into the system with 20 and 80 percent variations of the actual parameters. The saturation function $sat(s(t))$ is implemented to the system instead of $\mathrm{sgn}(s(\mathrm{t}))$ to restrain the chattering phenomenon. The control signal, the speed responses and the sliding surface for the conventional SMC and the DISMC for a step command (0-1400 rpm speed change) are shown in the following graphs.

In this situation, no matched uncertainty $\left(\tilde{N}=1\right)$ is taken for electromechanical system. The graphs of sliding surface, control input and speed of the system are plotted for the conventional SMC and the DISMC. The parameters are chosen to satisfy the requirements to be $c_1 = 50,\ c_2 = 0.5,\ \lambda = 250,\ \eta = 1.8 \times 10^9$. A step reference trajectory of 1400 rpm is applied to the control systems for all experiments. The sampling period is taken 2 ms for all conditions.

Figure. 0.2. Experiment Servo Motor Set

The tracking responses of the conventional SMC and the DISMC to a step references 1400 rpm are illustrated in Fig.5.3.a. and Fig.5.3.b. The performance of the system with the DISMC is much better than the system with the conventional SMC. The rise time and the settling time of the DISMC are also better. The settling time for the DISMC and SMC is approximately 0.15 s and 0.2 s, respectively. The conventional SMC has chattering effect, whereas the DISMC has nearly no chattering. No overshoot is observed for the conventional SMC and the DISMC. The DISMC has 15 rpm steady-state error, but the conventional SMC has a little larger about 25 rpm.

Control input signal for the conventional SMC and the DISMC are showed in Fig. 5.3.c. Control input for the conventional SMC has much more chattering than the DISMC. They converge nearly 0.2 s at the same time. Moreover, the input signal of two controllers stays with its bound of |2.5| V. Hence, the DISMC gives faster response than the conventional SMC.

The variations of sliding surface during the control for the conventional SMC and the DISMC are illustrated in Fig.5.3.d. and Fig.5.3.e. It is remarkable to say that the sliding function is $s(t) \neq 0$ when the error signal is not zero. The sliding signals reach to the sliding surfaces for the conventional SMC and the DISMC 0.2 s. The conventional SMC sliding surface converges to the origin with chattering, but the DISMC sliding surface converges exactly without nearly any chattering. However, the deviations and fluctuations of the conventional SMC are much more. They occur because of the uncertainties, errors and the disturbances. It is clearly inferenced from the Fig.5.3. that the deviations and fluctuations of the variations are smaller in DISMC control.

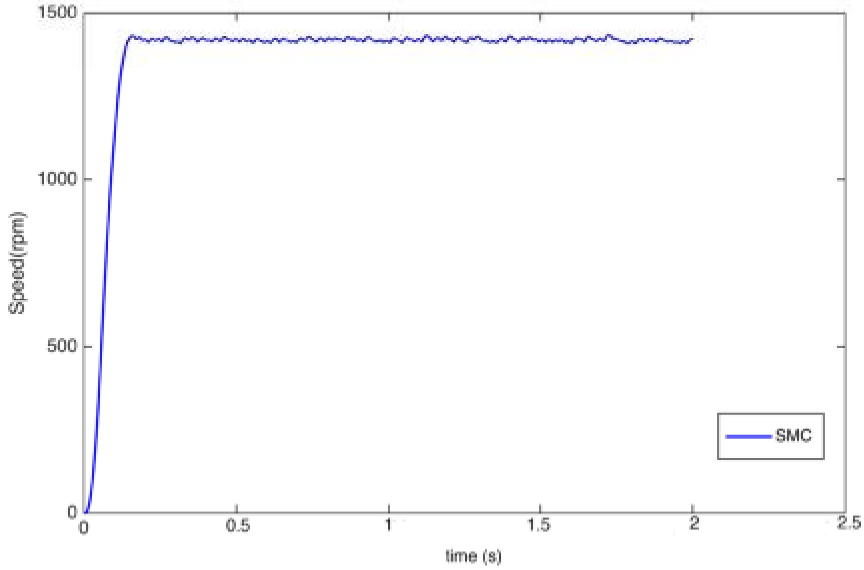
1500
1000
500
0
Speed(rpm)
0
0.5
1
1.5
2
2.5
time (s)
SMC

(a)

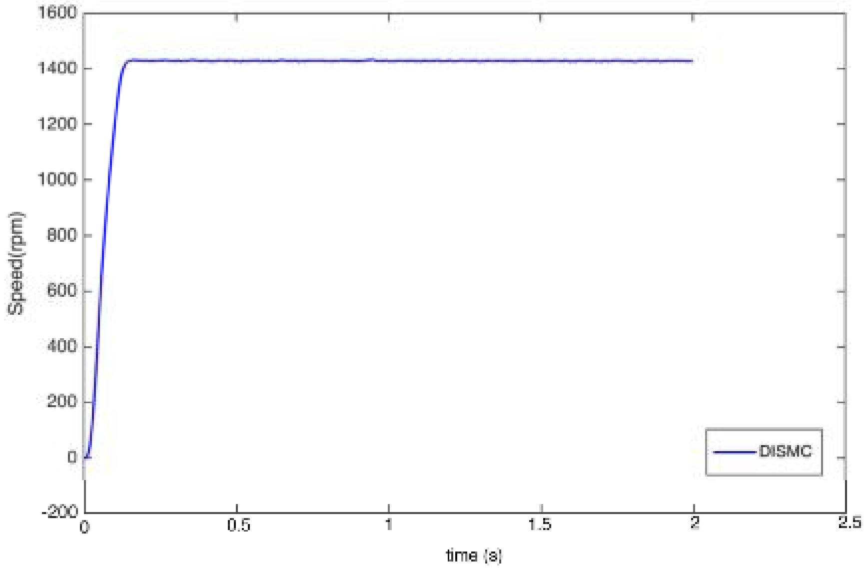
1600
1400
1200
1000
800
600
400
200
0
-200
Speed(rpm)
0
0.5
1
1.5
2
2.5
time (s)
DISMC

(b)

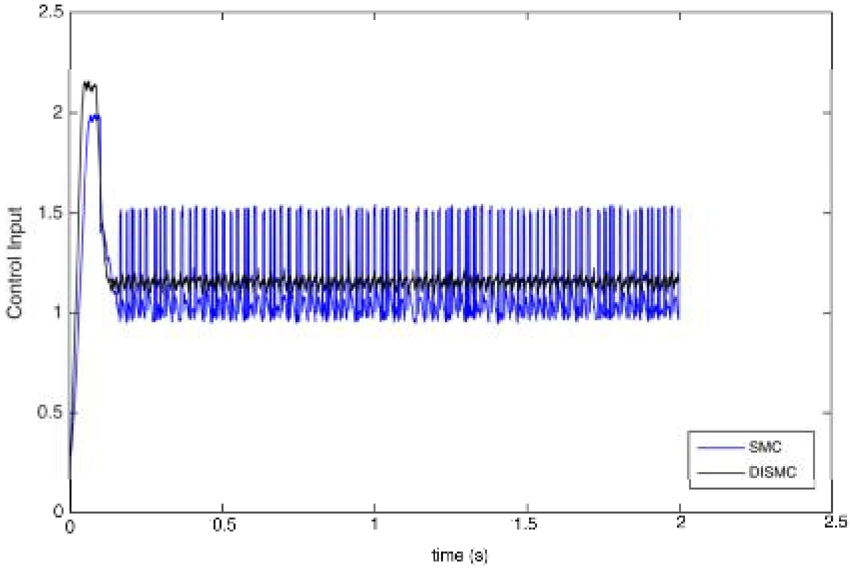

Control Input
time (s)
SMC
DISMC

(c)

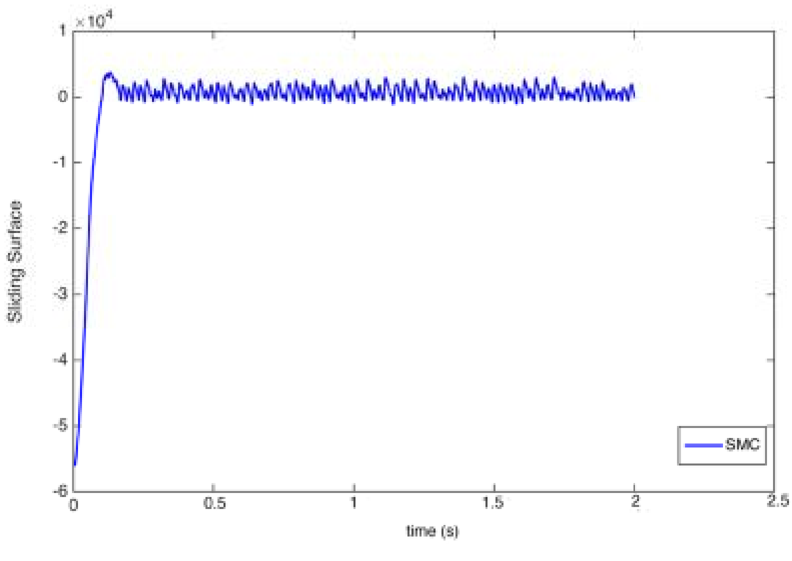

×10^4
Sliding Surface
time (s)
SMC

(d)

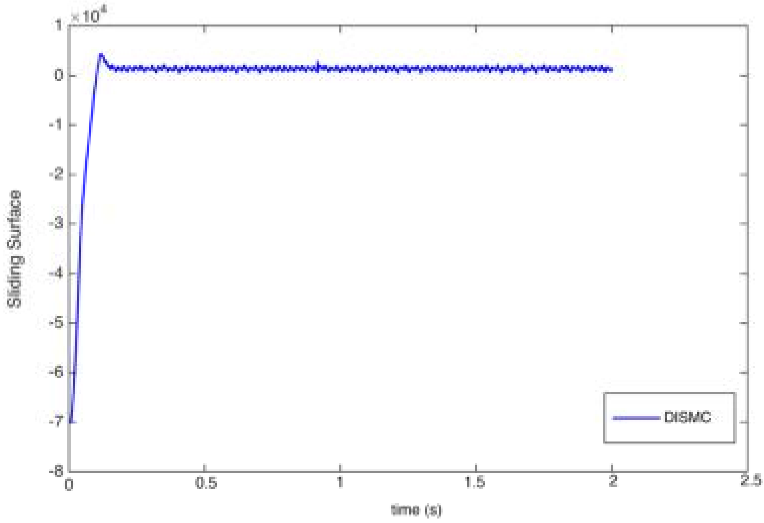

(e)

Figure. 0.3. Experimental Results for no uncertainty $\tilde{N} = 1$: (a) The Output Speed of the conventional SMC, (b) The Output Speed of the DISMC, (c) Control Inputs of the conventional SMC and the DISMC, (d) Sliding Surface of the conventional SMC, (e) Sliding Surface of the DISMC.

In this situation, the parametric uncertainty is introduced into the electromechanical system with 20 percent variations of the actual parameters $(\tilde{N} = 0.8)$. The parameters are chosen to satisfy the requirements to be $c_1 = 25,\ c_2 = 0.5,\ l = 18,\ h = 10^9$. The conventional SMC and the proposed control method (DISMC) are applied to the electromechanical system under this matched parameter uncertainty. The robustness of the conventional SMC and the DISMC are compared against the parameter uncertainty.

The output speed responses of the electromechanical system are shown in Fig.5.4.a. and Fig.5.4.b. for the conventional SMC and the DISMC. The output speed of the DISMC settles down at 0.15 s and the output speed of the conventional SMC settles down at 0.2 s. The system speed with the proposed controller (DISMC) is faster than those with the conventional SMC. The conventional SMC exhibits steady-state error about 40 rpm, but the DISMC displays the steady-state error about 15 rpm. The conventional SMC has chattering effect, but the DISMC has no chattering effect. There is no overshoot for the two controllers. The DISMC diminishes the reaching phase, has smaller raising time. The DISMC outperforms the conventional SMC at reducing chattering under the parameter uncertainty.

The control input signal variations are shown in Fig.5.4.c. for the conventional SMC and the DISMC. The conventional SMC displays much more oscillations than the DISMC with great magnitude in the presence of parametric uncertainty. These oscillations aren't as hazardous as chattering for the system, but still harm the actuators. The DISMC control effort is smoother than the conventional SMC and decreases the chattering by comparison with the conventional SMC.

The sliding manifolds for the conventional SMC and the DISMC are illustrated in Fig.5.4.d. and Fig.5.4.e. The conventional SMC sliding surface approaches to the origin with too much chattering, but sliding surface of the DISMC converges with less chattering than the conventional SMC. The settling time is almost equal for the conventional SMC and the DISMC. There is no overshoot for the conventional SMC and the DISMC. The sliding signal reaches to the sliding surface for the conventional SMC and the DISMC; however the deviation and the fluctations of the conventional SMC are much more than the DISMC.

The performance of the DISMC is much better than the conventional SMC. There is better rising time, has no overshoot and no chattering for the DISMC.

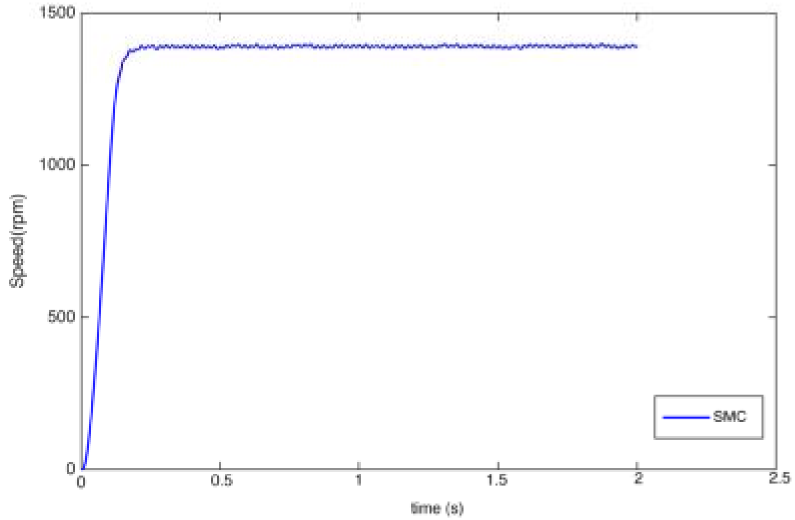
1500
1000
500
0
Speed(rpm)
0
0.5
1
1.5
2
2.5
time (s)
SMC

(a)

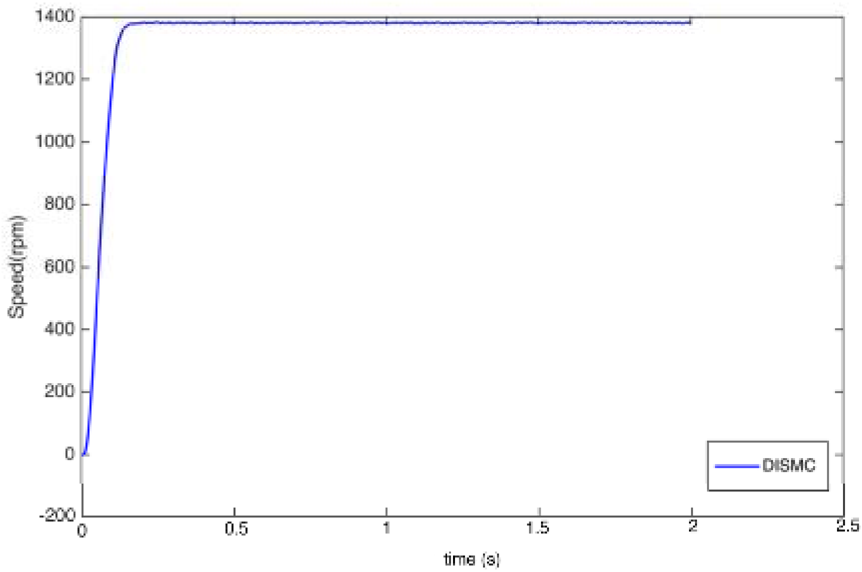
1400
1200
1000
800
600
400
200
0
-200
Speed(rpm)
0
0.5
1
1.5
2
2.5
time (s)
DISMC

(b)

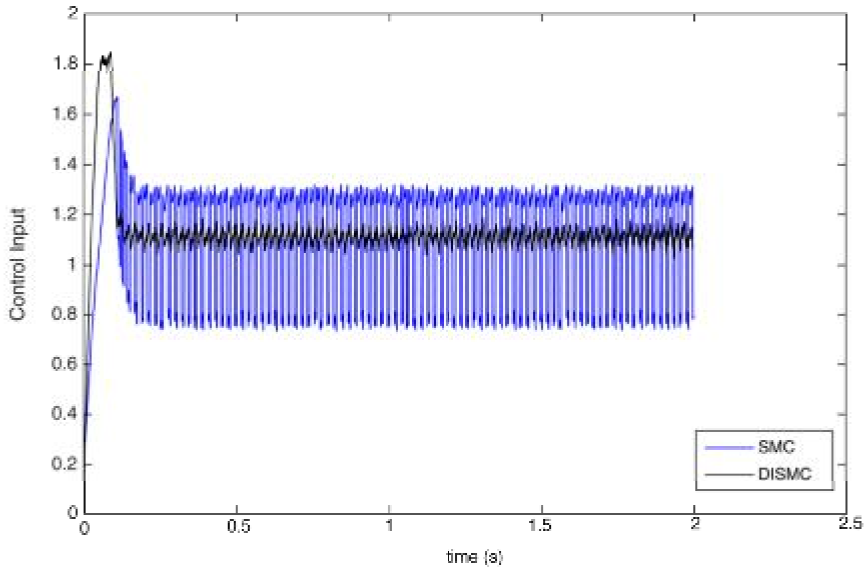

Control Input
time (s)
SMC
DISMC

(c)

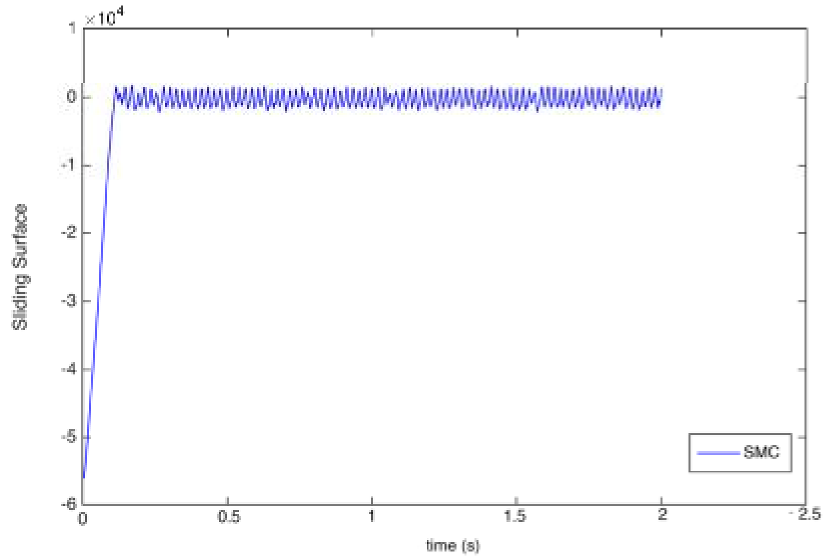

×10^4
Sliding Surface
time (s)
SMC

(d)

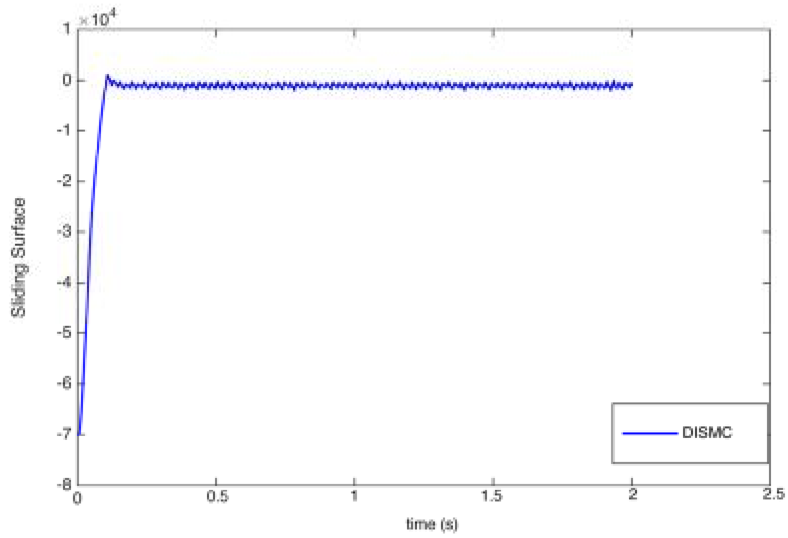

(e)

Figure. 0.4. Experimental Results for uncertainty $\text{Ñ} = 0.8$: (a) The Output Speed of the conventional SMC, (b) The Output Speed of the DISMC, (c) Control Inputs of the conventional SMC and the DISMC, (d) Sliding Surface of the conventional SMC, (e) Sliding Surface of the DISMC.

This last experiment with 80% of match uncertainty is done to make more certain remark on robustness of the DISMC and the conventional SMC $(\text{Ñ} = 0.2)$. The aim of this experiment is to display the robustness of the electromechanical system against the more disturbances and uncertainties, because there are always disturbances, noises and uncertainties in the real world systems. The purpose is to bring this system as close to real systems as possible. The parameters are chosen for this simulation to meet the conditions as $c_1 = 50,\ c_2 = 0.5,\ \text{l} = 200,\ \text{h} = 2´\ 10^9$. The difference between the performances of the controllers is increased in this situation.

The motor velocity responses of the electromechanical system are illustrated for the conventional SMC and the DISMC in Fig.5.5.a. The output speed of the DISMC and the conventional SMC settles down at 0.1 s in Fig.5.5.a. The system velocity with the proposed controller (DISMC) responds the same as those with the conventional SMC. The steady-state error is about 110 rpm for the conventional SMC and 30 rpm for the DISMC. The conventional SMC has chattering effect, but the DISMC has no chattering. There is no overshoot for the conventional SMC and the DISMC. The DISMC diminishes the reaching phase, has smaller raising time. The DISMC outperforms the conventional SMC at reducing chattering under the parameter uncertainty. The performance of the DISMC is much better than the conventional SMC. There is better rising time, no overshoot and no chattering for the DISMC.

The control input signals are illustrated for the conventional SMC and the DISMC in Fig.5.5.b. The conventional SMC displays oscillations with great magnitude in the presence of parametric variation. The DISMC control effort has also oscillations, but not as much as the conventional SMC and decreases the chattering when compared with the conventional SMC. The bound for the control signal is set to $|2.5V|$ for the electromechanical system. Both controllers are in these boundaries.

The sliding manifolds for the conventional SMC and the DISMC are shown in Fig.5.5.c. The sliding surface of the conventional SMC converges to the origin with great magnitude oscillations, but the sliding surface of the DISMC converges exactly without any oscillations. The settling time is almost eliminated with the DISMC. There is no overshoot for the DISMC and the conventional SMC. The sliding signal reaches to the sliding surface for only the DISMC; however the deviation and the fluctations of the conventional SMC are much more than the DISMC.

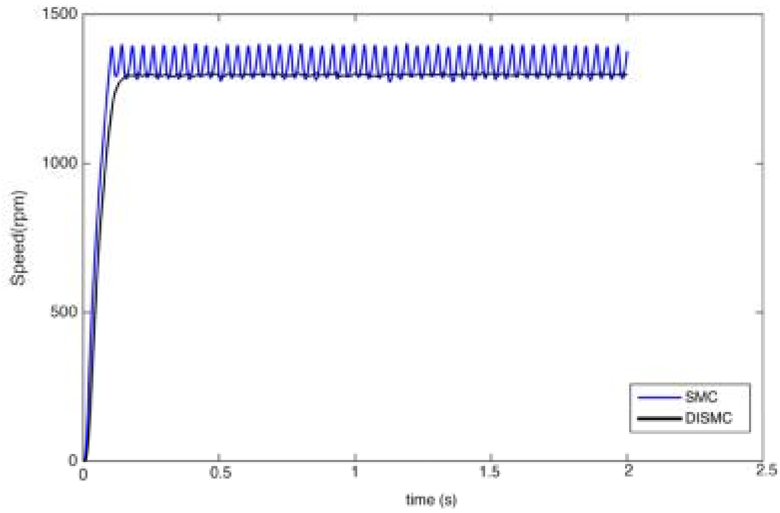
1500
1000
500
0
Speed(rpm)
0
0.5
1
1.5
2
2.5
time (s)
SMC
DISMC

(a)

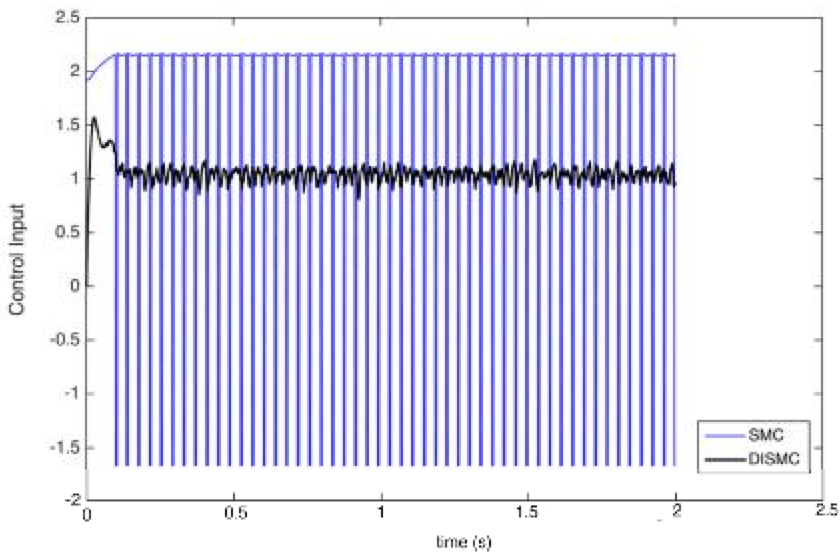
2.5
2
1.5
1
0.5
0
-0.5
-1
-1.5
-2
Control Input
0
0.5
1
1.5
2
2.5
time (s)
SMC
DISMC

(b)

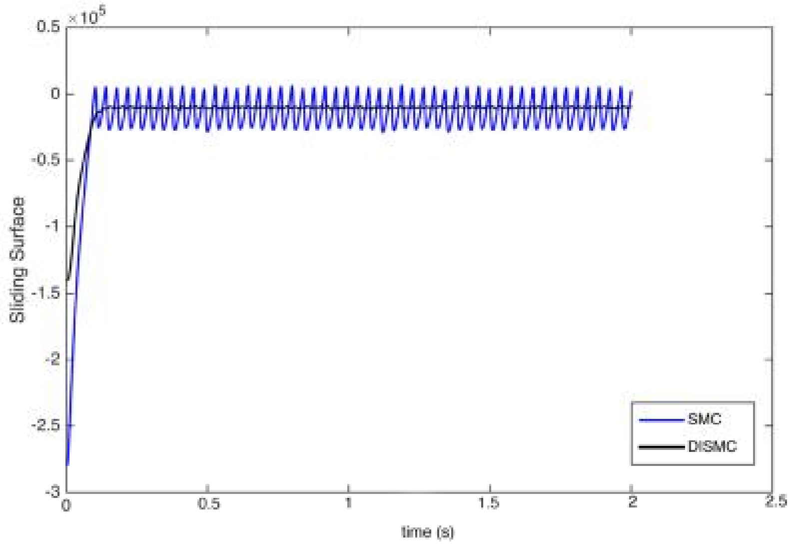

(c)

Figure. 0.5. Experimental Results for uncertainty $\tilde{N} = 0.2$: (a) The Output Speeds of the conventional SMC and the DISMC, (b) Control Inputs of the conventional SMC and the DISMC, (c) Sliding Surfaces of the conventional SMC and the DISMC.

The DISMC is more preferable for electromechanical systems in many control applications, because the conventional SMC may damage actuators in the systems.

The rise time, settling time, the overshoot time that are for the conventional SMC and the DISMC are illustrated in Table 2:

Table 5.1. The Characteristics of the Step Response

Controller type	Ñ	Rise time (ms)	Settling time (ms)	Overshoot
SMC	1	82.6	135.5	1.00
	0.8	96.2	167.7	0.54
	0.2	100.2	1997.3	1.86
DISMC	1	81.1	128.8	0.44
	0.8	79.4	134.1	0.11
	0.2	80.2	134.7	0.42

6. CONCLUSIONS

In this study, the Dynamic Integral Sliding Mode Control (DISMC) has been proposed to make the system control performance better, resolve uncertainty, chattering and external disturbances. Since many of the industrial systems use a DC servo motor, controlling of the speed and the position of the DC servo motor systems is required to give high accuracy; otherwise it damages the actuators and gives harm to system dynamics.

Firstly, the conventional SMC and the proposed DISMC design are emphasized by using a simulation program. The motor speeds, the system sliding surfaces and the control signals for the conventional SMC and the proposed DISMC are demonstrated with various parameter uncertainties. According to the simulation results, the DISMC is much more robust than the conventional SMC for eliminating chattering and removing overshoot under the matched uncertainty.

Then, some experimental applications of the conventional SMC and the DISMC are implemented to the real electromechanical system to show their effectiveness. The rotor speeds, the system sliding surfaces and the control signals for the conventional SMC and the proposed DISMC are investigated. Different uncertainty parameter values are applied to the system to test the robustness of the system.

According to the experimental results the conventional SMC doesn’t meet the needs of many systems. The DISMC is more efficient, robust against the parameter variations and smooth in the presence of the parameter uncertainty. The DISMC also overcomes the chattering phenomena. The tracking error for the DISMC converges to zero under the parameter uncertainties. The DISMC gives satisfactory temporary performance in terms of settling and rising time. It removes overshoot and makes the steady-state error minimum.

As a consequence, the DISMC is more efficient control method compared with the conventional SMC based on both a simulation program environment and the experimental results. Hence, the DISMC should be used in industrial systems alternatively because usage of it is simple, easy to implement, its robustness and performance are more effective than the conventional SMC. According to both the experimental results and a simulation program results, the robustness and the control performance of the system with the DISMC have been significantly increased.

REFERENCES

Aksu, I. O., and R. Coban. 2016. "Prediction of an Electromechanical System Parameters Using the Particle Swarm Optimization Algorithm." In *2016 IEEE 20th Jubilee International Conference on Intelligent Engineering Systems (INES)*, 85–88. https://doi.org/10.1109/INES.2016.7555098.

Aydin, M. N., and R. Coban. 2016. "Sliding Mode Control Design and Experimental Application to an Electromechanical Plant." In *2016 57th International Scientific Conference on Power and Electrical Engineering of Riga Technical University (RTUCON)*, 1–4. https://doi.org/10.1109/RTUCON.2016.7763076.

Chamsai, Tossaporn, Piyoros Jirawattana, and Thana Radpukdee. 2010. "Sliding Mode Control with PID Tuning Technique: An Application to a DC Servo Motor Position Tracking Control." *Energy Research Journal*, 55–61.

Chen, Dongbo, Haibo Du, and Xiaozheng Jin. 2017. "Position Tracking Control for Permanent Magnet Synchronous Motor Based on Integral High-Order Terminal Sliding Mode Control." In *Automation (YAC), 2017 32nd Youth Academic Annual Conference of Chinese Association Of*, 234–239. IEEE.

Coban, Ramazan. 2017a. "Adaptive Backstepping Control Design for Electromechanical Systems." In *Electrical and Computer Engineering (UKRCON), 2017 IEEE First Ukraine Conference On*, 267–270. IEEE.

Coban, Ramazan. 2017b. “Backstepping Sliding Mode Tracking Controller Design and Experimental Application to an Electromechanical System.” *Journal of Control Engineering and Applied Informatics* 19 (3): 88–96.

Coban, Ramazan. 2018. “Backstepping Integral Sliding Mode Control of an Electromechanical System,” 11.

Eker, İlyas. 2006. “Sliding Mode Control with PID Sliding Surface and Experimental Application to an Electromechanical Plant.” *ISA Transactions* 45 (1): 109–18. https://doi.org/10.1016/S0019-0578(07)60070-6.

Eker, İlyas, and Şule A. Akınal. 2008. “Sliding Mode Control with Integral Augmented Sliding Surface: Design and Experimental Application to an Electromechanical System.” *Electrical Engineering* 90 (3): 189–97. https://doi.org/10.1007/s00202-007-0073-3.

Fujisawa, S, Masanobu Obika, Toru Yamamoto, Kazuo Kawada, and O Sueda. 2004. *Speed Control of 3-Mass System with Sliding Mode Control and CMAC*. Vol. 5. https://doi.org/10.1109/ICSMC.2004.1401224.

Healey, A. J., and D. Lienard. 1993. “Multivariable Sliding Mode Control for Autonomous Diving and Steering of Unmanned Underwater Vehicles.” *IEEE Journal of Oceanic Engineering* 18 (3): 327–39. https://doi.org/10.1109/JOE.1993.236372.

Horng, Jui-Hong. 1999. “Neural Adaptive Tracking Control of a DC Motor.” *Information Sciences* 118 (1–4): 1–13. https://doi.org/10.1016/S0020-0255(99)00045-6.

Iqbal, M., A.I. Bhatti, and Q. Khan. 2009. “Dynamic Sliding Modes Control of Uncertain Nonlinear MIMO Three Tank System.” In *Multitopic Conference, 2009. INMIC 2009. IEEE 13th International*, 1–7. https://doi.org/10.1109/INMIC.2009.5383149.

Jang, Ming-Jyi, Chieh-Li Chen, and Cha’o-Kuang Chen. 2002. “Sliding Mode Control of Hyperchaos in Rössler Systems.” *Chaos, Solitons & Fractals* 14 (9): 1465–76. https://doi.org/10.1016/S0960-0779(02)00084-X.

Jiménez-Rodríguez, Esteban, Eliana Mejía-Estrada, Óscar Jaramillo-Zuluaga, and Juan D. Sánchez-Torres. 2016. “An Integral Sliding Mode Observer for Linear Systems.” In . International Federation of Automatic Control.

Koshkouei, A.J., K.J. Burnham, and A.S.I. Zinober. 2005. “Dynamic Sliding Mode Control Design.” *Control Theory and Applications, IEE Proceedings -* 152 (4): 392–96. https://doi.org/10.1049/ip-cta:20055133.

Li, Hongyi, Peng Shi, Deyin Yao, and Ligang Wu. 2016. “Observer-Based Adaptive Sliding Mode Control for Nonlinear Markovian Jump Systems.” *Automatica* 64 (February): 133–42. https://doi.org/10.1016/j.automatica.2015.11.007.

Li, Hongyi, Jiahui Wang, Ligang Wu, Hak-Keung Lam, and Yabin Gao. 2018. “Optimal Guaranteed Cost Sliding-Mode Control of Interval Type-2 Fuzzy Time-Delay Systems.” *IEEE Transactions on Fuzzy Systems* 26 (1): 246–257.

Liu, Jianxing, Sergio Vazquez, Ligang Wu, Abraham Marquez, Huijun Gao, and Leopoldo G. Franquelo. 2017. “Extended State Observer-Based Sliding-Mode Control for Three-Phase Power Converters.” *IEEE Transactions on Industrial Electronics* 64 (1): 22–31.

Perruquetti, Wilfrid, and Jean-Pierre Barbot. 2002. *Sliding Mode Control in Engineering*. CRC Press.

Sabanovic, Asif, Leonid M. Fridman, and Sarah K. Spurgeon. 2004. *Variable Structure Systems: From Principles to Implementation*. IET.

Shtessel, Yuri B., and Ilia A. Shkolnikov. 2003. “Aeronautical and Space Vehicle Control in Dynamic Sliding Manifolds.” *International Journal of Control* 76 (9–10): 1000–1017. https://doi.org/10.1080/0020717031000099065.

Slotine, J.-J. E., and Weiping Li. 1991a. *Applied Nonlinear Control*. Englewood Cliffs, N.J: Prentice Hall.

Slotine, J.-J. E., and Weiping Li. 1991b. *Applied Nonlinear Control*. Englewood Cliffs, N.J: Prentice Hall.

Tang, Rui, and Qi Zhang. 2011. “Dynamic Sliding Mode Control Scheme for Electro-Hydraulic Position Servo System.” *Procedia Engineering* 24: 28–32. https://doi.org/10.1016/j.proeng.2011.11.2596.

Utkin, V. I. 1978. “Sliding Modes and Their Applications in Variable Structure Systems.” *MIR, Moscow*. https://ci.nii.ac.jp/naid/10003097387/.

Utkin, V. I. 1993a. “Sliding Mode Control Design Principles and Applications to Electric Drives.” *IEEE Transactions on Industrial Electronics* 40 (1): 23–36. https://doi.org/10.1109/41.184818.

Utkin, V., and Hoon Lee. 2006. “Chattering Problem in Sliding Mode Control Systems.” In *International Workshop on Variable Structure Systems, 2006. VSS’06*, 346–50. https://doi.org/10.1109/VSS.2006.1644542.

Utkin, Vadim, Juergen Guldner, and Jingxin Shi. 2009. *Sliding Mode Control in Electro-Mechanical Systems, Second Edition*. CRC Press.

Utkin, V.I. 1993b. “Sliding Mode Control Design Principles and Applications to Electric Drives.” *IEEE Transactions on Industrial Electronics* 40 (1): 23–36. https://doi.org/10.1109/41.184818.

Vadim, I. Utkin. 1977. “Survey Paper Variable Structure Systems with Sliding Modes.” *IEEE Transactions on Automatic Control* 22 (2): 212–222.

Xue, W., and J. Li. 2016. “Robust Control of a Nonlinear Aeroelastic System Using Dynamic Integral Sliding Mode Control Method.” In *2016 35th Chinese Control Conference (CCC)*, 3351–56. https://doi.org/10.1109/ChiCC.2016.7553873.

CURRICULUM VITAE

Ebru ŞENYİĞİT SİNEKLİ was born in Mersin, in 1988. She completed the elementary education at Mersin, Turkey. She went to 19 Mayıs High School. She graduated from the Department of Mathematics, Anadolu University, Eskişehir, at 2011. She started to work as a teacher at MEB/Turkey in 2012. She completed MSc program at the Department of Computer Engineering in 2018.